NanoSpec

Nanomaterials for harvesting sub-band-gap photons via upconversion to increase solar cell efficiencies

Grant agreement no: 246200

Participant no.	Participant organisation name	Participant short name	Country	Principal Investigator
1 (CO)	Fraunhofer-Gesellschaft zur Förderung der angewandten Forschung e.V.	ISE	Germany	Jan Christoph Goldschmidt
2	Universität Bern, Departement für Chemie und Biochemie	UBE	Switzerland	Karl Krämer
3	Technion - Israel Institute of Technology	TEC	Israel	Efrat Lifshitz
4	Heriot-Watt University	HWU	United Kingdom	Bryce Richards
5	Forschungszentrum Jülich GmbH	IEF	Germany	Urs Aeberhard
6	Universiteit Utrecht	UU	Netherlands	Andries Meijerink
7	Philips Electronics Nederland B.V.	PH	Netherlands	Dick de Boer
8	Eindhoven University of Technology	TUE	Netherlands	Michael Debije

Summary

Silicon (Si) solar cells loose about 20% of the energy incident from the sun, because photons with energy below the band-gap are not absorbed in the silicon. Photon upconversion (UC) of sub-band-gap light is a promising approach to overcome this fundamental problem while still retaining the advantages of silicon photovoltaic devices. An upconverter generates one high-energy photon out of at least two low-energy photons. An additional up-converter pushes the theoretical efficiency limit from close to 30% up to 40% for a silicon solar cell illu-minated by non-concentrated light.

In the Nanospec project seven European partners joint their forces to develop an advanced upconverting system that significantly enhances solar cell efficiencies. Key developments were the upconverter material, the combination with a second luminescent material to enlarge the used spectral region, photonic structures for photon management and efficient solar cells.

Different lanthanide ions based upconverter materials were investigated to find the host lattice, the dopant and the dopant concentration that yielded the highest external UC quantum yield (eUCQY). Efficient IR to NIR UC was obtained for Er^{3+} in fluoride and oxysulfide hosts, while less efficient UC was obtained for Nd^{3+}, Sm^{3+}, Dy^{3+}, Ho^{3+} and Tm^{3+}. The material β-NaYF4 : 25% Er^{3+} with a particle size of 63-125 µm was identified as the best upconverter for broadband IR excitation. Improvements of the synthesis increased the eUCQY significantly by about 50%. As β-NaYF4 : 25% Er^{3+} is a microcrystalline powder, it needs to be incorporated into a transparent matrix for integration into an upconverter solar cell device (UCPVD). Perfluorocyclobutyl (PFCB) was found to be a good matrix material due its low optical losses, low polymerization temperature, suitable refractive index and good thermal stability.

As second luminescent materials, nano-crystalline semiconductor quantum dots (NQD) were investigated. The NQD should absorb the light, which is neither absorbed by the solar cell nor by the upconverter, and should emit in the absorption range of the upconverter. NQD with emission around 1520 nm und suitable absorption were realized as PbSe quantum dots (QD), PbS shell on PbSe core QDs, PbSeXS1-X alloy shells on PbSe QDs and PbSe-CdSe core-shell QDs. Synthesis with high chemical yield and amounts produced from one reaction in the range of 1-3 g could be realized. A very high, stable photoluminescence quantum yield (PLQY) of up to 25% was determined for PbSe-CdSe core-shell QDs in solution. Embedded in PFCB, the highest PLQY value found was around 20%. Furthermore, the absorption and PL spectra of ensembles of PbSe QDs and of PbSe-PbS core-shell QDs were simulated using a quantum-kinetic model.

Spectrally selective photonic structures were realized by plasma enhanced chemical vapor deposition of multi-layer structures from two different amorphous silicon carbides. A reflectance exceeding 95% and transmittance of up to 90% in the desired spectral regions was achieved. As

potential cheaper alternative, broadband reflectors based on cholesteric liquid crystals were investigated.

Adapted bifacial microcrystalline Si thin-film solar cells, with optimized contact grid configuration, and adapted bifacial monocrystalline wafer-based Si solar cells, with optimized anti-reflection coatings on front and rear, were produced. In such a configuration, the predicted short-circuit current density of the solar cell of 40.6 mA/cm^2 was modelled to increase by 1.5 mA/cm^2 by adding a realistic Er-based upconverter in conjunction with idealized NQD under one sun-illumination.

We realized experimentally planar, bifacial monocrystalline n-type Si solar cells with optimized ARCs. UCPVDs were formed by coupling embedded upconverter materials to the solar cells. For an UCPVD, in which β-NaYF4 : 25% Er^{3+} embedded in PFCB with a powder to polymer concentration of 75.7 w/w% was coupled to the solar cell, an additional short-circuit current density due to UC of sub-band-gap photons $\Delta J_{SC,UC}$ of 2.2 ±0.3 mA/cm^2 was determined under broadband excitation ranging from 1450 nm to 1600 nm and an equivalent solar concentration of 78±6 suns. In solar simulator measurements a $\Delta J_{SC,UC}$ of 13.3 ±3.0 mA/cm^2 was achieved for a concentration of 207±86 suns. This is the highest $\Delta J_{SC,UC}$ value determined so far.

Taking a broader picture into account, we could show that the materials used in the Nanospec system are relatively abundant, and the concept is not limit by resource availability. Furthermore, procedures were developed to safely handle all involved materials. A cost analysis showed that Er-based upconverters have the potential to increase the cost efficiency of a concentrator module.

As a conclusion, the realized upconverter devices and also its components achieved world record performance levels. However, the impact of upconversion on the device performance is still relatively low. As a consequence, the concept is still not commercially viable. Based on our results, however, we estimate that with additional research it should be possible to realize devices, in which upconversion increases the efficiency of a 23% efficient silicon solar cell to up to 25% thereby increasing the cost-efficiency of such systems.

Project context and the main objectives

In the Nanospec project (Nanomaterials for harvesting sub-band-gap photons via upconversion to increase solar cell efficiencies) novel nanotechnology-based materials and structures were developed, new concepts explored and knowledge generated, all with the common goal to manufacture silicon solar cells with higher efficiencies by utilizing upconversion of low-energy photons. Higher efficiencies are essential to continue the path of cost reduction in photovoltaics with a long-term perspective. The project is therefore an important contribution to ensure the wide dissemination of photovoltaics (PV), to improve the sustainability of the European energy supply structure, to reduce environmental hazards like global warming, and to strengthen and improve the economic situation of the European PV industry, and the European economy as a whole. The proposal investigated the novel concept of upconversion of photons with energies below the band-gap of silicon, which was made possible by the innovative use of photonic nanostructures and nanotechnology-based materials.

With a market share of around 90%, silicon wafers are the dominant material for the production of solar cells. Two key advantages of silicon result in this dominating position: its non-toxicity and its abundance. Innovation in the past was mainly focussed on reducing production costs. However, reducing production technology costs makes material costs increasingly important. Currently about 50% of the module costs can be accounted for by material costs [1]. The strategic answer to this situation is to increase the efficiency of the solar cells. With higher efficiencies, more kWh can be produced from the same amount of silicon. Overall, the system costs are reduced due to more efficient use of space and the reduced consumption of material, electricity, and resources. To reduce the amount of involved resources is a critical challenge, not only from a cost perspective, but also to lower the amount of resources needed to meet our energy demands.

Consequently, new cell concepts are being developed to increase silicon solar cell efficiencies. Already, above 20% efficiency can be reached in industrial production[2,3]. However, the maximum efficiency achievable with silicon solar cells is limited by fundamental loss mechanisms to less than 30%. Around 35% of the incident power is lost because the energy of the photons exceeding the bandgap of silicon is transformed into heat.

1 C. del Canizo, G. del Coso and W.C. Sinke, Prog. Photovolt: Res. Appl.; 17:199-209 (2009)

2 E. Maruyama et al., Proc. 4th World Conf. PV Energy Conversion, Waikoloa, Hawai, USA (2006)

3 D. De Ceuster et al., Proc. 22nd EUPVSEC, Milan, Italy (2007)

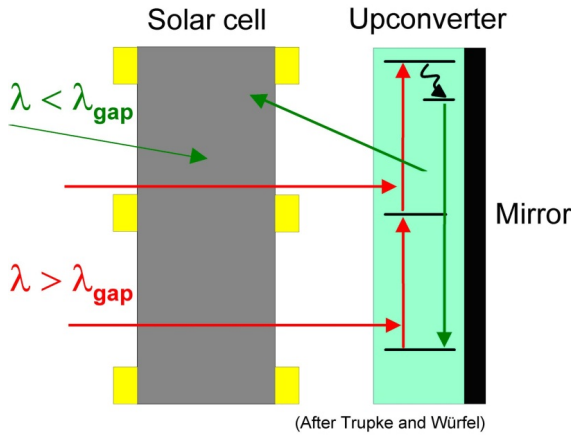

Fig. 1: Bifacial solar cell with an upconverter on its rear side. Sub-band-gap photons are transmitted through the solar cell but absorbed in the upconverter which is excited successively. By recombination to the ground state, the upconverter emits a photon which can be absorbed by the solar cell.

Very suitable as upconverters are rare earth based materials, like $NaYF_4:Er^{3+}$ [4]. Rare earths, especially trivalent erbium, exhibit energy levels which are very conveniently spaced for upconversion for silicon solar cells. The host material for the erbium should have low maximum phonon energies, to reduce the loss due to non-radiative decay. $NaYF_4$ is an ideal host-material fulfilling this condition. The major problem of rare earth based upconverters like erbium doped $NaYF_4$ is the weak and narrow absorption range of the rare earth dopant. To overcome this limitation, the upconverter can be combined with a luminescent material [5]. The luminescent material should absorb all photons with wavelengths between the band-gap of the solar cell and the absorption range of the upconverter and emit in the narrow absorption range of the upconverter. Because the solar photon density over a broad spectral range is funnelled to a smaller range, we call this process spectral concentration. This approach increases upconversion efficiency significantly by two mechanisms [6]: firstly, more light is absorbed that is potentially upconvertible. Secondly, the photon density in the absorption range of the upconverter is increased. Upconversion is a nonlinear process. The relationship between incoming radiation and emission is described by a power law. For the investigated material, the relationship is roughly quadratic. With doubled excitation, the emission is increased four-fold. PbSe and PbS nanocrystal quantum dots (NQD) are ideal candidates as luminescent material. They show strong absorption in the required spectral range and a very efficient emission at lower energies. NQD with a core from PbSe and a graded shell of a PbSe and PbS alloy have especially good properties [7,8,9,10]. Similarly, HgTe NQDs

[4] K.W. Krämer, D. Biner, G. Frei, H.U. Güdel, M.P. Hehlen, S.R. Lüthi, Chem. Mater. 16, 1244 - 1251 (2004)

[5] C. Strümpel et al., Proc. 20th EUPVSEC Barcelona, Spain (2005)

[6] J.C. Goldschmidt, P. Löper, S. Fischer, S. Janz, M. Peters, S. W. Glunz, G. Willeke, E. Lifshitz, K. Krämer, D. Biner, IUMRS-ICEM08, Sydney, Australia (2008)

[7] M. Brumer, A. Kigel, L. Amirav, A. Sashchiuk, O. Solomesch, N. Tessler, E. Lifshitz, Adv. Fun. Mater., 15, p. 1111 - 1116 (2005)

which may also be capped with wider bandgap semiconductors like CdS and CdTe are an excellent choice.

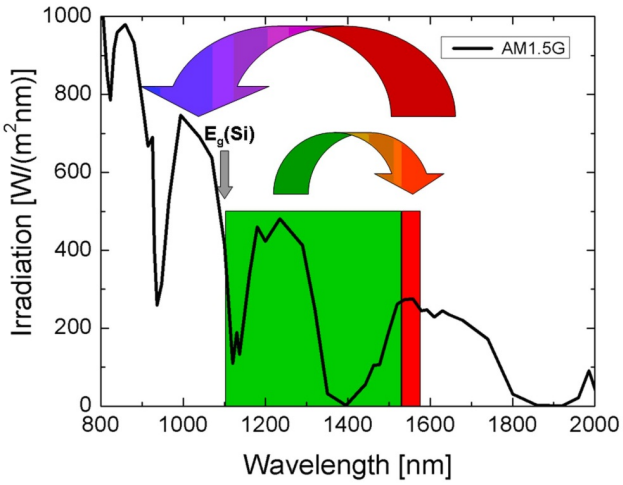

Fig. 2: Spectral concentration and upconversion. The fluorescent material absorbs in a broad spectral range (1100 nm - ca. 1520 nm) and emits in the absorption range of the upconverter (around 1540 nm). The upconverter emits photons with energies above the band-gap EG of the silicon solar cell.

An additional increase in illumination intensity and therefore efficiency can be achieved by additional geometric concentration; that is, by collecting light from a large area and concentrating it on a smaller area. Concentration with lenses and mirrors is already well known. In this project we also investigated the concentration within the upconverting device with the use of fluorescent concentrators [1112]. The internal concentration can be used in addition to an external concentration. The fluorescent concentrator is formed by incorporating the luminescent NQD into a transparent material [13] or on top of it [14]. Total internal reflection or reflective structures trap most of the emitted light inside the concentrator. The light can only escape where the upconverter is optically coupled to the concentrator. When the upconverter does not cover the complete back of the solar cell, the infrared radiation from the complete cell area is concentrated onto the small area of the upconverter.

---

[8] E. Lifshitz, M. Brumer, A. Kigel, A. Sashchiuk, M. Bashouti, M. Sirota, E. Galun, Z. Burshtein, A. Q. Le Quang, I. Ledoux-Rak, and J. Zyss, J. Phys. Chem. B, 110(50), p. 25356 - 25365 (2006)

[9] A. C. Bartnik, F. W. Wise, A. Kigel, E. Lifshitz, Phys. Rev. B, 75, p. 245424 (2007)

[10] A. Kigel, M. Brumer, G. Maikov, A. Sashchiuk, E. Lifshitz, SMALL, in press (2009)

[11] J. C. Goldschmidt, P. Löper, M. Peters, Deutsches Patent, Bundesrepublik Deutschland, Fraunhofer-Gesellschaft zur Förderung der angewandten Forschung e.V. 10 2007 045 546 (2009)

[12] T. Kirchartz, J. Mattheis, U. Rau, Phys. Rev. B, 78, p. 235320 (2008)

[13] J. Mattheis, J. H. Werner, U. Rau, Phys. Rev. B, 77, p. 85203 (2008)

[14] R. Bose et al., ., Proc. 22nd EUPVSEC, Milan, Italy (2007)

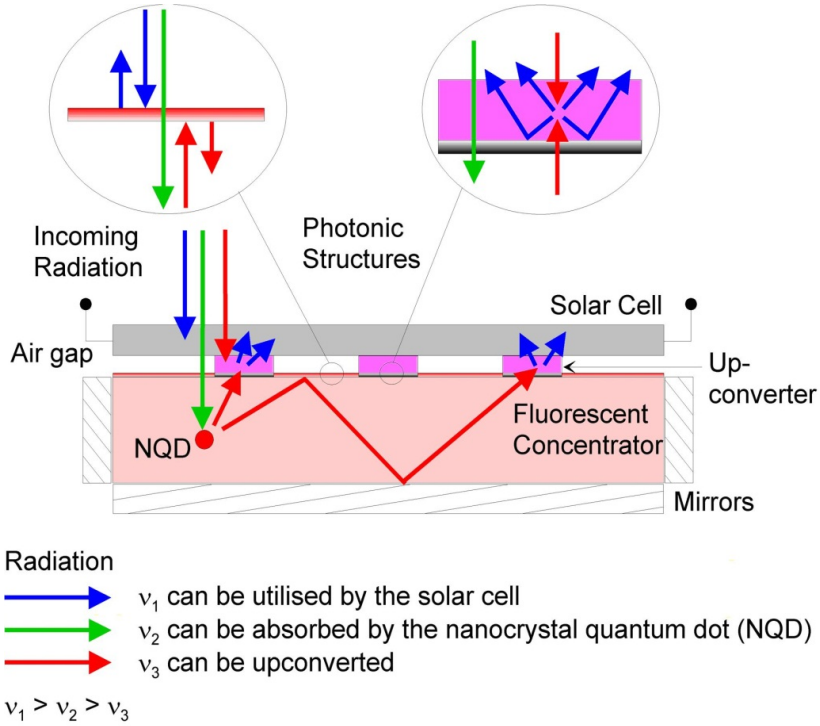

Fig. 3: Setup of an advanced upconverter system [15] that was investigated in this project. The solar cell absorbs photons with energies above the band-gap (ν1). Photons with less energy are transmitted (ν2, ν3). The upconverter transforms especially low energy photons (ν3) into high energy photons that can be used by the solar cell (ν1). Photons with energies below the band-gap but above the absorption range of the upconverter (ν2) are absorbed by the nanocrystal quantum dots (NQD), which emit photons in the absorption range of the upconverter (ν3). The emitted radiation is guided by total internal reflection and/or photonic structures to the upconverter. As the upconverter does not cover the whole area, a geometric concentration is achieved. Radiation which is emitted from the upconverter towards the fluorescent concentrator is back reflected by a spectrally selective photonic structure. A patent has been granted for this concept.

Photonic structures (with varying properties) are used for several purposes in the setup. The first purpose is to prevent the radiation emitted by the upconverter from re-entering the fluorescent concentrator: the aforementioned NQD also absorb the radiation emitted from the upconverter. Thus upconverter and fluorescent material must be separated from each other and the upconverted radiation should be prevented from entering the fluorescent concentrator again. This is done with selectively reflective photonic structures placed between fluorescent concentrator and upconverter.

[15] J.C. Goldschmidt, P. Löper, S. Fischer, S. Janz, M. Peters, S. W. Glunz, G. Willeke, E. Lifshitz, K. Krämer, D. Biner, IUMRS-ICEM08, Sydney, Australia (2008)

The second purpose is to increase the collection efficiency of the fluorescent concentrator and to be a good back reflector for the silicon solar cell. A third purpose could be to integrate either the luminescent NQD or the upconverter into a photonic structure to achieve higher efficiencies via resonance effects.

The presented concept integrates progress in several disciplines into a very advanced photovoltaic device. In comparison with other advanced photovoltaic device concepts, it has a high realisation potential, because it relies on well-established silicon solar cell technology and just adds electronically passive optical layers. This is a clear advantage over other systems, which interfere with the electronic properties of the solar cell device (e.g. impurity photovoltaic devices or intermediate band solar cells). Moreover, because of this "add-on" characteristic, the concept can be applied to other photovoltaic technologies, like the different emerging thin-film technologies or future technologies that are currently being developed.

Objectives

It was our overall objective to realize a complete system with all the mentioned components, which shows a significantly higher efficiency than a silicon solar cell alone in the three years of the project, which results into the potential for cost reduction. In the end, lab-scale prototypes were tested outdoors integrated into concentrator modules. Furthermore, it was one key objective to prepare the exploitation of the project results in the form of a commercial product in the context of the consortium. To achieve these goals, the project created significant progress in the science and technology of nanostructures and nanotechnology-based materials.

The following detailed list of objectives was pursued:

- The theoretical modelling and simulation of the important dynamics and processes.
- Development of highly efficient, near-infrared emitting luminescent nanocrystalline quantum dots (NQD).
- Development of highly efficient upconversion phosphors.
- Development of highly energy selective, high reflection, high transmission photonic structures for photon management.
- The implementation of upconverters and nanocrystals in new matrix materials.
- The development of both crystalline and thin-film silicon solar cells that are highly efficient adapted to the use of upconverted light.
- The integration of all components into one system and testing these systems outdoors integrated into a concentrator module.
- To ensure the impact of the project in the European photovoltaic industry, a roadmap for the further exploitation was developed. Furthermore, the abundance of the involved materials was investigated and a life-cycle analysis performed.

Main Scientific results

Theoretical modelling and simulation

The fluorescent-concentrator upconverter system that was to be designed and realized in the Nanospec project represents a complex system formed by a number of innovative and technologically challenging components. Each of these functional components was to be investigated theoretically in a separate modelling step and the resulting descriptions were eventually to be integrated into a comprehensive simulation of the overall system performance. In this way, a deeper understanding of the fundamental mechanisms of the photon-conversion process should be gained, suitable configurations be defined for the implementation of functional component structures and the performance of these implementations be assessed for further optimization.

For the different optimization tasks, it was important to be able to simulate the behaviour of the most important novel component of the device, the upconverter material. Therefore, one tasked aimed at the development of a predictive rate equation model for the upconversion process. The comprehensive simulation developed for this task includes the processes of ground and excited state absorption, stimulated and spontaneous emission, relaxation via coupling to lattice vibrations, as well as transfer of energy between up-converter atoms. The Einstein coefficients for the radiative transitions were determined experimentally. The model was successfully validated by comparing the dependence of the upconversion efficiency on irradiance with the corresponding experimental data. The model was further extended to describe upconversion under broadband illumination. To this end, a model was developed to reproduce the spectral line broadening of the upconverter material due to electric field induced splitting of the atomic levels.

The second material that needed to be described, were nanocrystal quantum dots (QD) used as luminescent species for the sensitization of the upconverter material via spectral concentration of the near-infrared radiation. Since the luminescent behaviour of an accumulation of these tiny objects with substantial variation in size and shape deviates considerably from that of a conventional crystalline volume material, a novel theory for QD luminescence was developed and applied to ensembles of nanocrystals synthesized, taking into account the microscopic processes occurring in the quantum dots from the absorption of the broad spectrum of near infrared light passing through the solar cell to the stimulated and spontaneous emission of the characteristic spectrum according to the composition, size and shape of the quantum dot. While a true quantitative reproduction of experimental spectra remains challenging, the new approach provides a sound qualitative picture of physical line shape and spectral shifts due to interaction of optical, electronic and vibrational degrees of freedom. The formalism was applied to investigate the fluorescence spectra of spherical and egg-shaped PbSe-PbS core-shell nanocrystal quantum dots.

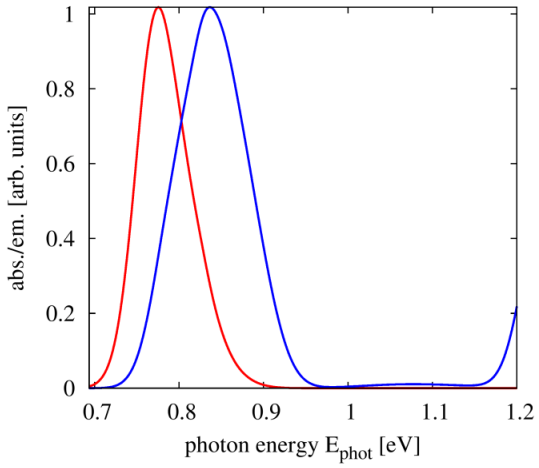

Fig. 4: Simulated Absorption and photoluminescence spectra of a spherical PbSe-PbS core-shell QD under non-resonant (broadband) excitation, with consideration of fast relaxation processes.

A third task, was dedicated to the simulation of photonic structures, for both the design of spectrally selective filters required to confine the convertible frequencies in the solar cell and the near-infrared part in the concentrator module, and the investigation of a potential enhancement of the upconversion efficiency via the exploitation of resonance effects in specially designed optical cavity structures. The filter design was realized using an evolutionary optimization algorithm in conjunction with a tool for the simulation of absorption, transmission and reflection of dielectric layer stacks. The procedure resulted in the identification of photonic structures exhibiting very high spectral selectivity, which was confirmed by the experimental realization of the structures.

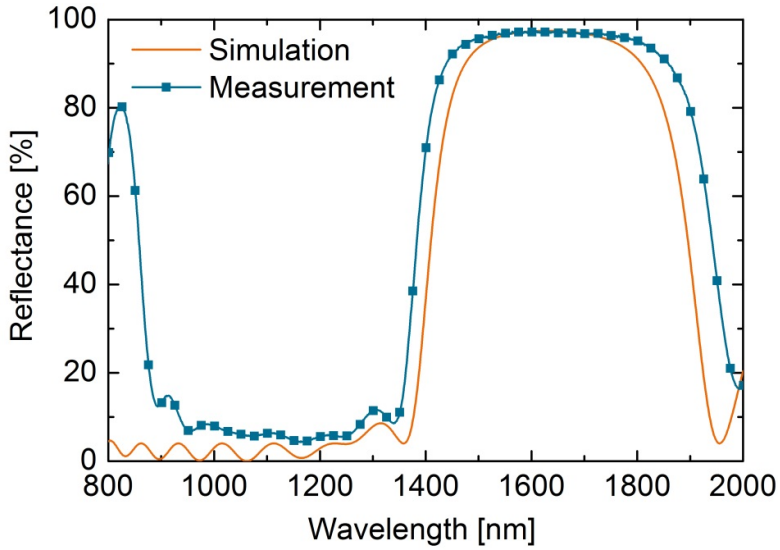

Fig. 5: Simulated and measured reflectance of multi-layer amorphous SiC nano-structures with high spectral selectivity.

As an exploratory side topic, the use of micro-cavities, formed by the spectrally selective photonic structures containing upconverter material, to increase upconversion efficiency was investigated. The impact of the micro-resonator effects was assessed using different methods for the rigorous numerical solution of Maxwell's equations for the determination of the electromagnetic mode and field density for a given dielectric cavity structure and coupling this results to the intensity-dependent rate equation model for the upconversion process. In this way, an overall increase of the upconversion quantum yield of close to a factor of two was determined for a simple dielectric cavity structure.

Besides the luminescent materials, and the photonic structures, also the silicon solar cells needed to be adapted. Therefore, bifacial silicon solar cells optimized for transmission of the light with energy below the absorption threshold of the active solar cell material were modelled. In the case of the thin film silicon solar cell, the standard tool used for amorphous and micro-crystalline silicon solar cell device simulations was complemented with a model for transparent front and back contacts with metal grid configuration, taking into account optical and electrical losses in these functional layers, and a phenomenological model for the concentrator-upconverter device, which transforms the transmitted sub-gap spectrum into a monochromatic backside illumination at the main luminescence frequency of the upconverter material. The results of the optoelectronic contact optimization procedure were used to guide the fabrication of thin film silicon solar cells for use with the near-infrared concentrator-upconverter system. However, the simulations also revealed that the potential increase of the overall conversion efficiency provided by the bifacial design with upconverter is marginal for thin-film silicon solar cells. In the case of the crystalline silicon solar cell, a combination of a commercial 3D optoelectronic device simulator with a similar phenomenological model of the concentrator-upconverter was devised. The optical model, based on ray-tracing and including the backside illumination from the upconversion process, was used to determine optimal anti-reflection coatings for front and backside illumination spectra. In an optimized configuration, the predicted short-circuit current density of the solar cell of 40.6 mA/cm^2 was modelled to increase by 1.5 mA/cm^2 by adding a realistic Er-based upconverter in conjunction with idealized nanocrystalline QD (NQD) under one sun-illumination.

As final task, an optical simulation of the fluorescent concentrator module and an overall assessment of the possible device performance was performed. For this purpose, a ray-tracing simulation was extended to include the absorption and subsequent emission from the luminescent species, i.e., the nanocrystalline quantum dots. This analysis established that the nanocrystalline quantum dots have to fulfil very high demands in terms of absorption, emission bandwidth and photoluminescence quantum yield.

Development of Upconverter Material

Upconversion (UC) is a process where several photons are absorbed in a material followed by the emission of one photon at higher energy. In literature mainly monochromatic excitations are discussed, e.g. by laser light, and an approximate resonance between the excitation steps is an important condition. But in the Nanospec project the excitation energy originates from the infrared part of the solar spectrum and comprises a wide range of wavelengths. Such conditions require new UC materials adapted to these low power density, multi color excitation conditions. Since several photons are required in the excitation process, an UC material needs multiple meta-stable energy levels which act as reservoirs for the excitation energy. Such conditions can be found for rare earth ions RE^{3+} with their partially filled 4f electron shells, e.g. Er^{3+}.

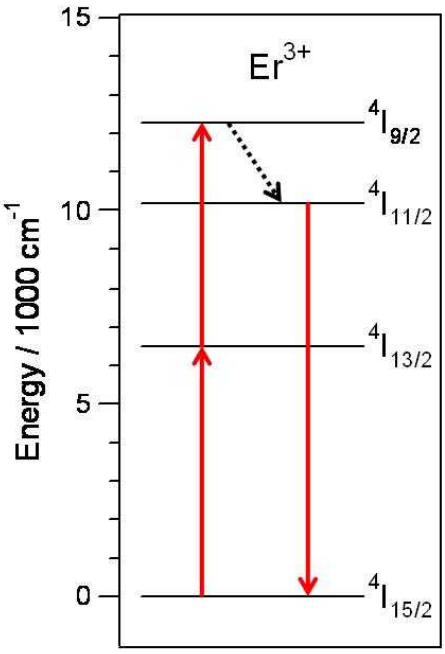

Fig. 6: Energy level diagram of the upconverter material Er^{3+}.

The properties of the meta-stable states are determined by their energy gap and life time. The energy gap is the energy difference of a state towards the next, lower lying state. According to the energy gap law, a state is called meta-stable if the energy gap is bigger than at least five times the maximum phonon energy of the host lattice. For smaller energy gaps the excitation energy is converted into phonons, i.e. lost as heat. On the contrary, a meta-stable state can store the energy for a certain time, its life time. The life time is defined as the time in which the population of a state decays towards $1/e \approx 0.3679$. Long life times in the order of 10 ms are found for the $^4I_{13/2}$ and $^4I_{11/2}$ states of Er^{3+} in fluoride lattices, whereas the $^4I_{9/2}$ state quickly relaxes to the $^4I_{11/2}$ state due to its small energy gap. The meta-stable states can emit their energy as a photon or undergo further interactions. In the case of Er^{3+}, an emission from the $^4I_{11/2}$ state is ideally suited for the excitation of an electron across the band gap of silicon, i.e. the creation of an electron-hole pair in Si which

can generate a current in the solar cell. On the other hand, an excitation in the $^4I_{13/2}$ state is an intermediate in the UC process. Two Er^{3+} ions, both excited into their $^4I_{13/2}$ state, can interact with each other and exchange their energy. In this process, one Er^{3+} ion takes up the energy and is excited to the $^4I_{9/2}$ state whereas the other one relaxes to its ground state. Such a process is called energy transfer UC (ETU) and is the dominant UC process in the materials discussed here.

In order to find the best UC material for the Nanospec project, the host material, the dopant ion, and the dopant concentration were optimized. All samples were characterized by X-ray diffraction for their phase purity. Their UC efficiency was monitored in a powder test set-up. Here, the infrared part (λ>1300 nm) of the broad band emission from a W-lamp was filtered off by a Si- and a dielectric long-pass filter. This infrared light was focused on the sample and the upconverted emission measured by a Si-detector. The powder test set-up closely resembles the excitation by sub-Si-band-gap photons from the solar spectrum. It allows a quick and reliable screening of a big number of samples as obtained from the synthetic work.

The host lattice is an important part of the material since it determines the relevant maximum phonon energy. This phonon energy should be low in order to avoid energy losses by multi phonon relaxation as discussed above. Furthermore, the host lattice has to provide suitable sites for the dopant ions, preferably of the same charge and size. During the project many lattices were tested of which β-$NaYF_4$ turned out as the best choice. This host lattice is well known for very efficient visible UC. It offers two rare earth sites with nine-fold coordination and microscopic disorder. The absence of an inversion center at the metal site and the broadening of the line width due to the disorder are the main reasons for its superior properties. Its maximum phonon energy of about 350 cm^{-1} is extraordinary low for a fluoride and significantly lower than in any oxides. Due to the existence of α-$NaYF_4$, a high temperature polymorph with distinctly worse optical properties, the synthesis of β-$NaYF_4$ is chemically demanding. But the synthesis of β-$NaYF_4$ could be optimized during the project in order to obtain phase-pure, oxygen-free material with highest UC efficiency.

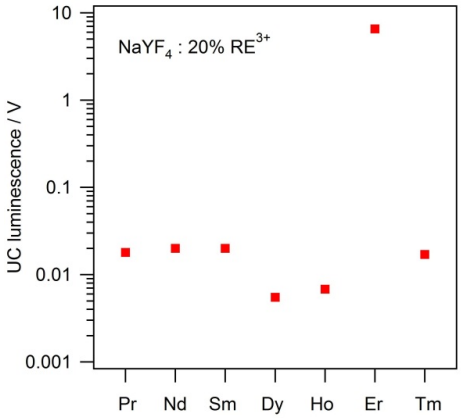

Fig. 7: Upconversion luminescence signal of different of upconverter materials with different dopant ions. Er^{3+} clearly shows the most intense upconversion.

Among the possible dopant ions, all rare earth ions with energy levels in the suitable infrared spectral region were tested. Out of those the Er^{3+} ion clearly showed the best upconverion properties for broad band infrared excitation with low power density. It was more than two orders of magnitude superior to others. In a concentration series, β-$NaYF_4$ samples with 0 to 100% Er were synthesized. The UC efficiency quickly goes up with the Er doping and shows a maximum around 25 to 30% Er. For higher concentrations the efficiency declines slowly due to concentration quenching. Therefore, β-$NaYF_4$:25% Er was identified as the best UC material for the Nanospec project.

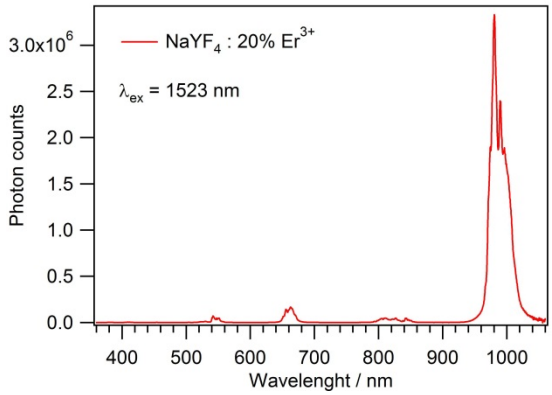

Fig. 8: UC emission spectrum of β-$NaYF_4$:Er for 1523 nm excitation.

It shows the dominant $^4I_{11/2} \rightarrow {}^4I_{15/2}$ Er^{3+} emission around 1000 nm which is ideally suited for the excitation of silicon. Depending on the Er concentration and the excitation power, the $^4I_{11/2}$ emission contains 95-98% of all emitted photons. This emission is excited in a two step ETU process. It constitutes the simplest and most efficient UC process. The $^4I_{9/2} \rightarrow {}^4I_{15/2}$ Er^{3+} emission around 800 nm originates from the same two photon process and adds about another 1% of the photons. Also the $^4S_{3/2} \rightarrow {}^4I_{15/2}$ and $^4F_{9/2} \rightarrow {}^4I_{15/2}$ Er^{3+} emissions around 540 and 660 nm, respectively, contain about 1% of the emitted photons, each. They are due to three photon UC processes. These emissions create electrons in the solar cell, but they are less efficient due to the higher order process. The UC efficiency of the material does not only depend on the Er^{3+} concentration and the excitation power, but also on the particle size. An optimum was observed for about 100 µm size particles. Coming from larger particles, the increase of the UC signal with decreasing particle size is due to a denser packing of the material in the sample tubes. For the smallest size fraction the efficiency decreases again due to an increasing number of broken crystallites and a higher surface to volume ratio.

After the optimum UC material was identified with respect to composition, particle size, and synthetic parameters, a bigger amount of material was produced for prototype production.

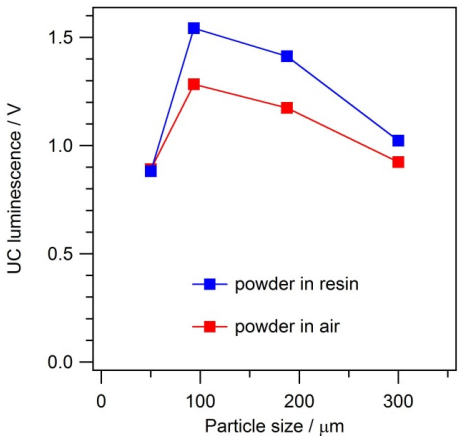

Fig. 9: Strength of the upconversion luminescence for different particle sizes.

Development of luminescent nanocrystralline quantum dots

One of the core activities of the Nanospec project was the synthesis and characterization of colloidal quantum dots (CQDs), acting as light harvester - absorbing a wide spectral range of the sun light, however emitting in the near infra-red (NIR) regime. The goal was, to develop luminescent QD that show the right spectral properties, a high quantum yield of the absorption and emission process, are chemically yield and can be produced a large amount weith efficient processes. We focused on the synthesis of CQDs from the IV-VI semiconductor family (e.g.,PbSe and PbS). These CQDs exhibit characteristic quantized electronic states and variable band-gap energy in the NIR spectral regime, upon the change of the of the CQDs' size. Further on, inter-band optical transitions in IV-VI CQDs possess relatively high absorption coefficient however, they do show some limitation regarding photo-chemical stability. This limitation was overcome by the formation of core/shell structures, comprised of a PbSe core, covered by an epitaxial layer of another semiconductor, such as small band-gap PbS, a wide band-gap CdSe, or a shell with an alloy composition.

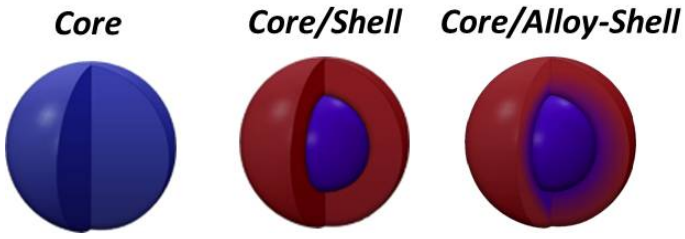

Fig. 10: Scheme drawing of quantum dots with core (left) core/shell (middle) and core/alloyed-shell (right) composition.

The specific composition was selected in order to enable high quality epitaxial growth with a crystallographic mismatch < 3%, enabling high quality core/shell interface (with defect-free surfaces). The synthesized core/shell CQDs: PbSe/PbS, PbSe/CdSe or PbSe/$PbSe_xS_{1-x}$ CQDs also showed additional fine tunability of the band-gap energy with variation of the core-to-shell volume division or/and composition. Further on, the synthesized CQDs (core and core/shell) are covered by organic surfactants, enabling further processing; e.g., embedding them in polymer films.

The following paragraphs outline the main synthesis efforts. The structural and composition properties of the produced CQDs were carried out by common techniques (transmission electron microscopy [TEM] X-ray diffraction, X-ray photo-electron spectroscopy, energy dispersive analysis of X-ray). The optical properties were characterized by recording the absorption, emission, quantum efficiency and lifetime, either at room temperature or at variety of temperatures. For the compression of the picture, a few observations will be given here.

The main effort in this work package was to deliver chemically stable CQDs operating at an appropriate wavelength to pump the Er-NPs up-converters; viz. the formation of core/shell CQDs. However, the key effort started with the synthesis of core PbSe-CQDs at various sizes, with a high emission quantum yield (mostly depend on the crystallographic and surface quality). CQDs are formed by injection of reagents (hereon called precursors) into a mother solution, mostly at elevated temperatures (70°C – 180°C). The mother solution contains functional molecules (hereon called ligands) playing a major role during the growth process in avoiding aggregation, and eventually remain as surfactants on the CQDs' surface. The most common synthesis utilized Pb-oleate ($Pb(OA)_2$) and trioctylphosphine-selenium (TOP:Se) as the precursors, which produced PbSe-CQDs with emission quantum efficiency of ~ 40%. However, very quickly we discovered that their chemical yield is ~ 5%, substantially below the requirements of the project. Thus, at an earlier stage than planned, we merged into the efforts to up-scale the synthesis procedure, by adding diphenylphosphine (DPP) to the reaction solution enhancing the reaction rate.

In an next step PbSe/PbS core/shell CQDs were synthesized. The initial efforts in the formation of PbSe/PbS utilized PbSe-core CQDs based on TOP:Se precursor. It involved precipitation of the core-CQDs from their mother solution and re-dispersion into a new solution (free of the Se monomer). Then, an injection of Cd- and S- precursors at stoichiometric amounts for a shell layer were injected into the pre-prepared cores at elevated temperature. TOP:S was used as the S-precursor. In the spirit of the discussion above, most reagents were replaced due to the low reactivity, which led to a slow generation of nuclei and low chemical yields. Then, PbSe cores were synthesized by the high-chemical yield route involving enhancement with an addition of DPP. Also, TOP:S was replaced by bis(trimethylsilyl)sulfide (TMS_2S) for the shell coverage.

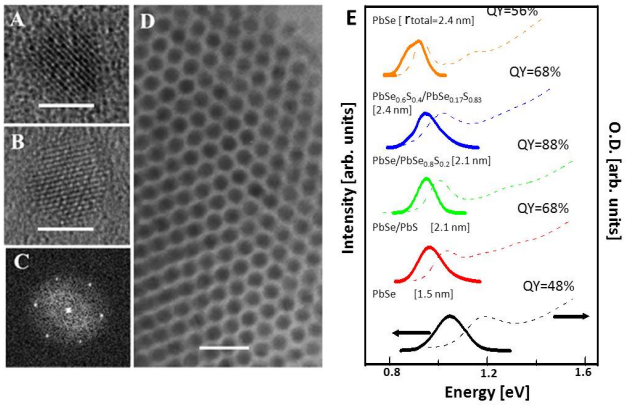

Fig. 11: TEM images of individual PbSe core (A) and PbSe/PbS core/shell (B) CQDs (scale bar= 5 nm), and corresponding electron diffraction of PbSe cores (C). TEM image of assemble of PbSe/PbSexS1-x CQDs (scale bar=12 nm), designating size uniformity. Absorption and emission spectra of CQDs as marked on the panel with average radius as indicated in the brackets. The emission quantum yield (QY) is indicated as well.

Chemical stability was measured by monitoring the stability of the luminescence intensity over a while temperature range (4K to 300K), with/without exposure to air for a certain period of time (up to 80 minutes). Core/shell materials showed higher stability than the simple cores.

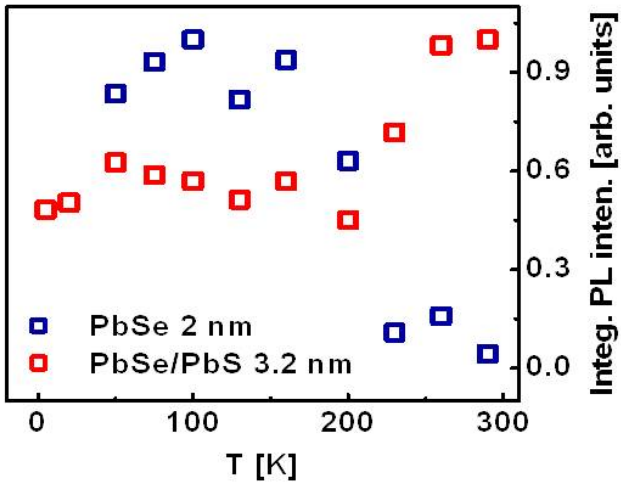

Fig. 12: Plots of the integrated emission intensity versus the measured temperature (T) of PbSe core (average radius 2 nm) and the corresponding PbSe/PbS core/shell CQDs. The plot designate a quench of the emission at elevated temperatures in bare PbSe cores, presumably due to oxidation, however retain of the emission efficiency in the case of core/shell structures by the shell protection.

Alternatively, also PbSe/CdSe core/shell CQDs were synthesized. An advantage of using PbSe/CdSe core/shell CQDs is the existence of relatively large energy gap between absorption and

emission energy, enabling minimization of re-absorption. PbSe/CdSe core/shells have been prepared using an cation-exchange reaction. The as-prepared PbSe CQDs are placed in a mixture of octadecene and Cd-oleate (~0.1M). The Pb in the PbSe is replaced by Cd, creating a core/hell structure with the same outer dimensions and shape as the original PbSe CQD, but with a smaller core. The shell thickness can be influenced by changing the concentration of the Cd-precursor, the reaction time and the temperature. For a longer reaction time the photoluminescence shifts to shorter wavelengths, due to a decreasing size of the PbSe core at longer exchange times.

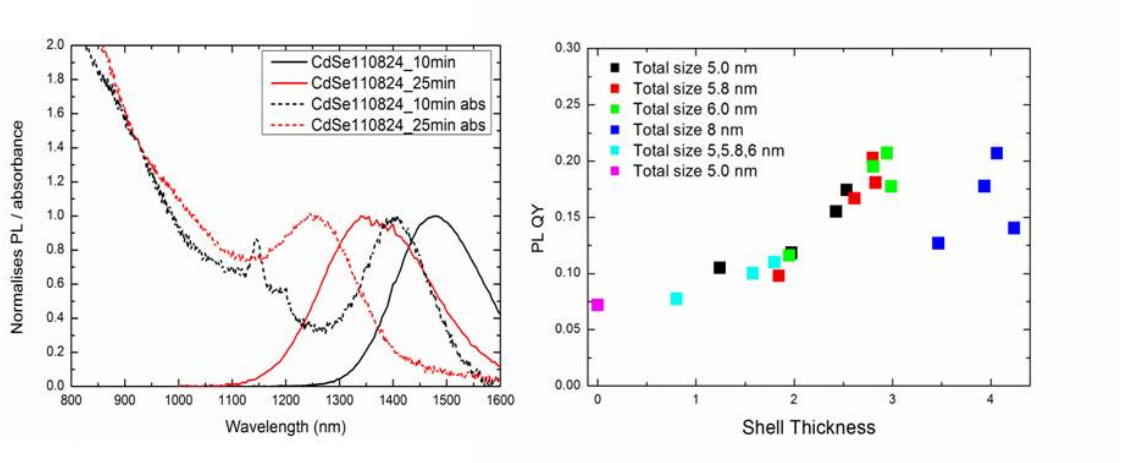

Fig. 13: Quantum Yield (left) of PbSe|CdSe core|shell particles with various shell thicknesses and corresponding PL spectra (right).

The quantum yield (QY) in respect to the shell-thickness was investigated to optimize the efficiency. With increasing shell thickness the absolute QY, measured with an integrating sphere, was increased from ~10% for PbSe NCs to 20-25% for PbSe/CdSe CQDs with a shell thickness of approximately 3 nm. Any further growth of the shell thickness, reduced the QY value. The photoluminescence lifetimes of these samples were also measured. While the PbSe sample has a single exponential decay, the core/shell samples all have a bi-exponential decay and longer lifetimes. Also noteworthy is the apparent longer long lifetime when a thicker shell is grown, suggesting a reduction of carriers overlap, typical to type-II alignment between core and shell constituents. The maximum QY of 25% is higher than previously reported in the literature for PbSe/CdSe CQDs, but probably below the optimal value for IR-luminescent concentrator. Several different methods were explored to raise the QY, including shell growth with different materials, i.e. CdS, CdS/ZnS, ZnS, ZnSe and combinations of these shells, to protect the surface and reduce surface losses. Various growth techniques were used, e.g. SILAR (standard and at lower temperature and different chemicals), Ion exchange and by using single source precursors (Zn-ddtc (ZnS) and Cd-ddtc (CdS)). However, all these synthesis, yielded either unstable CQDs (although with QYs up to 35%) or CQDs with a lower QY.

Finally, also PbSe/$PbSe_xS_{1-x}$ core/ alloyed-shell CQDs were investigated. The formation of core/alloyed-shell CQDs utilized two different routes:

(a) Co-injection of all precursors (Pb, Se, S) into a single pot at 130°C, using TOP:Se and TOP:S as precursors: The observations revealed a formation of PbSe pure core-CQDs in the initial time of the reaction, due to the large difference in reactivity of TOP:Se and TOP:S. However, in the following stage more and more PbS is deposited on the CQDs, since the TOP:Se is almost completely consumed. The QY of PbSe/$PbSe_xS_{1-x}$ produced in this manner were the best to achieve (60-80%). Unfortunately, the co-injection procedure suffered from a low chemical yield (5%), which is a drawback for the current project.
(b) Pre-preparation of PbSe CQDs followed by a separate process for the growth of the shell: As a 1st attempt, we used a mixture of TMS_2Se and TMS_2S for the growth of an alloyed shell. However, this strategy led an increase of the size distribution. Therefore we developed an alternative coating procedure using DPP:Se and DPP:S, allowing us to maintain a sharp size distribution, when adding 0.5 monolayer (half unit-cell) of PbS or $PbSe_XS_{1-X}$ on top of PbSe-CQDs by an alternating addition of the anion (DPP:Se/DPP:S) and cation (Pb^{2+}) precursors. Prior to the synthesis process, a thorough study using ^{31}P-NMR spectroscopy confirmed the bounding of DPP:Se and DPP:S to PbSe-CQD exterior surfaces.

The syntheses discussed, emanated CQDs capped by oleic acid (OA). The as-prepared CQDs were directly used to embed them in polymer films andcould be homogeneously dispersed in the polymer without a requirement for further modification of the ligand. Still, capping exchange experiments were performed (e.g., exchange with a variety of amines (from hexylamine to hexadecylamines) and different acids (e.g., hexanoic acid and hexadecanoic acid) to investigate the influence on the QY for PbSe QDs and PbSe/CdSe core/shell QDs.

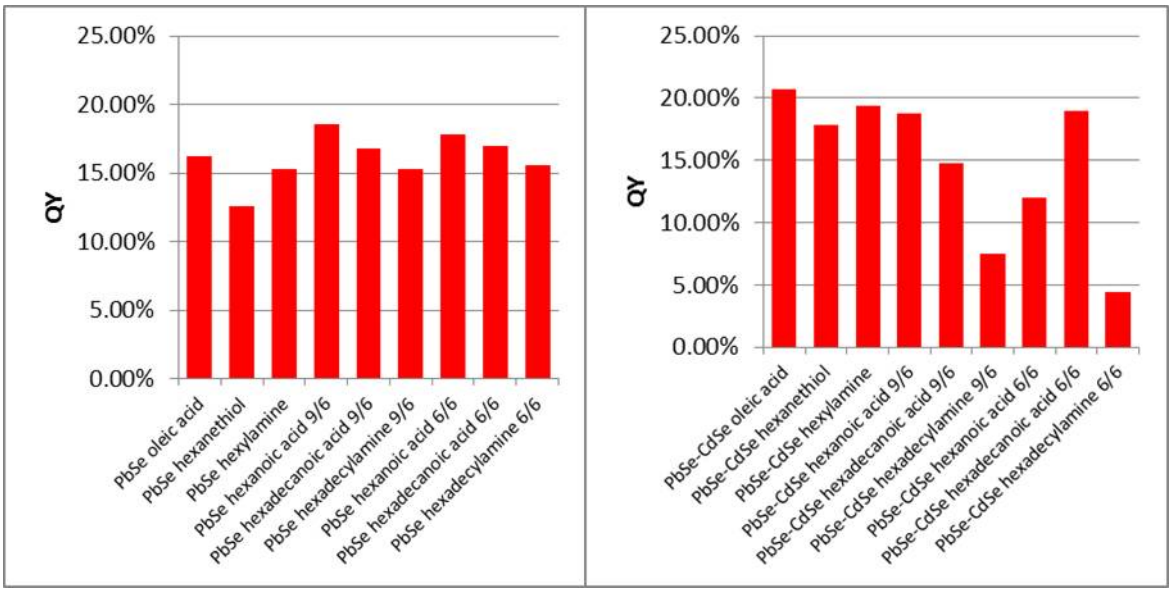

Fig. 14: Quantum yields measured for PbSe and PbSe/CdSe QDs with different capping ligands

The highest QY was obtained for the original oleic acid capped PbSe/CdSe CQDs. A modification of the ligand shell was not necessary as the oleic acid capping provides CQDs with optimum QY that can be homogeneously dispersed in perfluorocyclobutane (PFCB) polymer.

To warrant an efficient utilization of the invested chemicals, to supply sufficient materials for the following stages in the project, and to achieve a prove of concept for up-scaling option in commercial application, the up-scaling of the different synthesis methods was investigated. The efforts were initiated by the optimization of the chemical reaction of the core growth (keeping the volume of the reaction vials), hence, maximizing the use of the injected precursors.
The PbSe-CQD synthesis, we followed the high-chemical yield procedure using reaction enhancement by DPP.

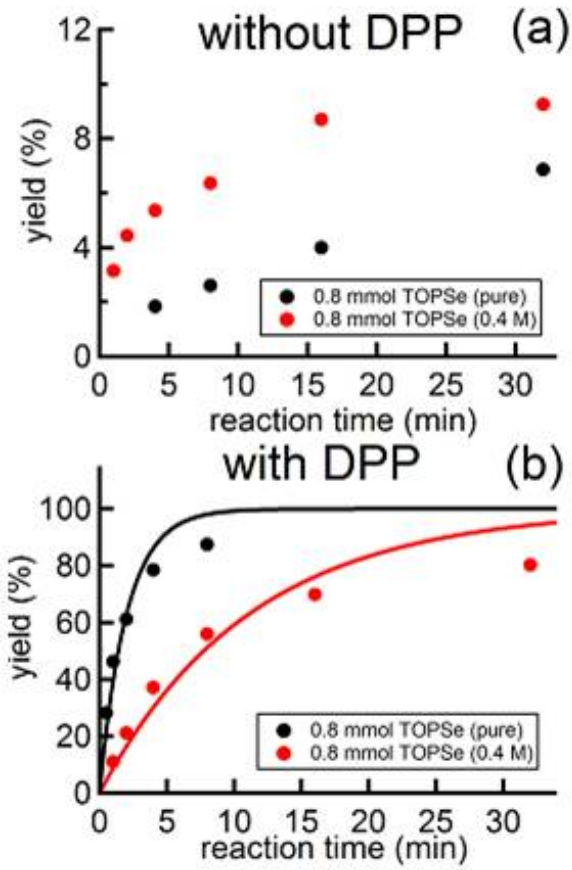

Fig. 15: Plot of the chemical yield versus the reaction time (min) for a reaction based on PbSe(oleate) and TOP:Se, without (panel a) and with (panel b) addition of DPP. Each panel also compares reaction solution with excess TOP (red symbols) or elimination of excess TOP (black symbols), revealing the inhibiting process of free TOP. Thus, optimal growth conditions include mixer of TOP:Se+DPP in the absence of excess TOP.

Following this synthesis, the cation loading in the reaction mixture was enhanced from about 5 % to 20 % relative to the previous syntheses, while keeping a reaction volume of about 13 ml. This allowed us enhancing the absolute reaction yield by ~ a factor of 10 up to 450 mg with a reaction yield close to unity. The absorption wavelength could be adjusted by the concentration of the anion precursors, which were used in excess. Finally, performing the reaction under the same conditions like before, but enhancing all amounts by a factor of 6, we were able to produce about 2.8 g of PbSe CQDs in a 100 ml flask. This result was later applied in an automated system, with a better control of reproducibility and on-line monitoring of the absorption.

Up-scaling of the procedure discussed for the growth of PbSe-shell using TMS_2S was not a straight forward process (facing obstacle related to the hydrolysis of TMS_2S by minor water reminiscence). To avoid this reaction, the reaction mixture was dried by a more sophisticated purification procedure, repelling water impurity by adding hexadecylamine . Finally, the initial reaction mixture was up-scaled by a factor of 15, allowing the synthesis of about 2 g of the desired material could be prepared in a 250 ml flask.

Up-scaling experiments for PbSe CQDs core, used later for a cation exchange with Cd (to produce PbSe/CdSe core/shell CQDs), initially was based on Pb-oleate and TOP:Se in a mixture of Diphenyl Ether (DPE) and TOP. This common synthesis supplied a relatively low chemical yield (35 nmol, ~0.05g of ~6 nm particles). To scale up the yield, a synthesis involved the use of Sn-precursor ($Sn[N(SMe)_3)_2]_2$) to create SnSe CQDs which are in-situ exchanged by Pb in an oleylamine mixture. The yield per synthesis volume of this synthesis is much higher than that of the standard procedure, however in some circumstances small CQDs (~2 nm) are also observed alongside the desired size, especially when the size of the CQDs exceeds 5 nm. Hence, a third synthesis method was used, using a Pb-oleate precursor (in octadecene) and a TOP:Se precursor, as well as a small amount of DPP to catalyse the reaction (similar to the latest trend used in WP6.1). The main advantage (besides the fact that it is a ‘greener’ synthesis) is a higher yield per reaction volume (~800 nmol per synthesis, ~6 nm CQDs) than the other syntheses, while still a good size-control is achieved. Typical product yields are now ~1 g of PbSe CQDs, as a starting point for the formation of PbSe/CdSe

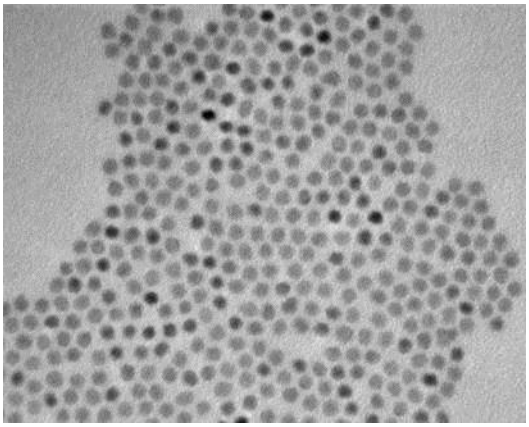

Fig. 16: Monodisperse 6 nm PbSe QDs synthesized using upscaling method with diphenylphosphine to enhance the reaction rate, giving product yields of ~1000 mg of PbSe CQDs.

Development of spectrally selective photonic structures with high reflectance

Spectrally selective photonic structures are required in the Nanospec system to guide the photons according to their energy into the part of the device where they are utilized most efficiently. Two different filter structures are required for this application: the filter sitting directly below the upconverter, the upconverter (UC) filter, has to reflect upconverted photons, thus, photons in the absorption range of a silicon solar cell. For all other wavelengths, this filter should have a high transmittance in order to allow photons in the absorption range of the upconverter to reach this material and those in between to reach the luminescent concentrator. A second filter, the spectral-concentration (SC) filter that is applied in the regions where no upconverter is placed has a second task: it has to reflect photons in the absorption range of the upconverter, thus, those photons can be guided to the upconverter material.

In order to produce these two spectrally selective filters, two different approaches were investigated: first, photonic structures based on amorphous silicon carbides (a-SiC_x) deposited in a plasma-enhanced chemical vapor deposition (PECVD) process and second, the use of cholesteric liquid crystals.

The a-SiC_x-filters rely on the fact that the refractive index of the material can be tuned with the silicon to carbon ratio, generally, the higher the silicon content, the higher the refractive index of the layer. Using PECVD this ratio can be influenced by the relative gas-flows of methane and silane. For this work, a low-refractive index layer was obtained for gas flow rates of 110 sccm methane and 7 sccm silane. This layer has a refractive index of 1.7. For the high-refractive index layer, the gas flow rates were set to 40 sccm methane and 60 sccm silane which resulted in a refractive index of 2.3. Layers with higher silicon content, thus, higher refractive index, tend to have an island-like growth and thus, cannot be used for the formation of thin closed homogeneous

layers. In the PECVD chamber, argon plasma was used to split the compounds, which was powered by pulsed microwaves. This resulted in a more homogeneous layer deposition than the deposition with continuous-wave microwaves and a radiofrequency source.

Using these developed processes, layers of different refractive indices could be obtained and characterized by ellipsometry. These experimental values were taken as a base for transfer matrix simulations to optimize the layer thicknesses for the desired filter characteristics. Starting from simple Bragg-filters, the layer thicknesses were changed in order to match the requirements with as few layers as possible.

These optimized filter structures were then deposited and a peak reflectance of 95% and a peak transmittance of 90% in the respective regions could be obtained.

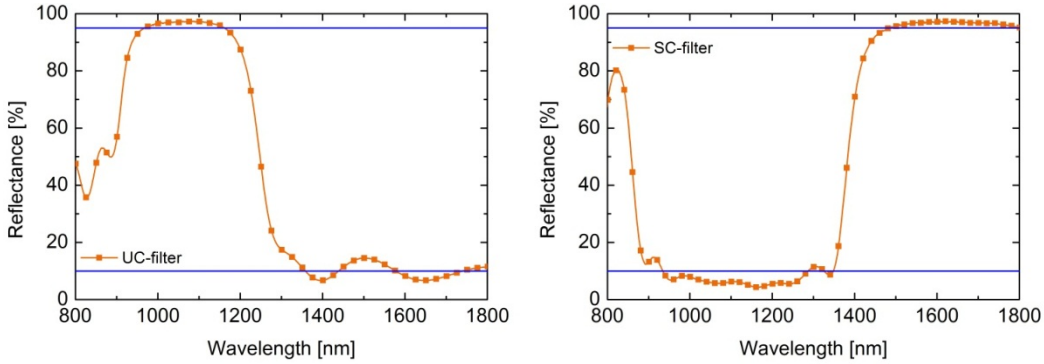

Fig. 17: Reflectance spectra of the realised SiC photonic structures showing the high spectral selectivity and high reflectance in the desired spectral regions.

While inorganic materials can be used to form excellent selective reflectors for use in the Nanospec device, they have the disadvantage of being quite time consuming and expensive to produce on a large scale. Generally, they require sequential depositing of nanometer thick layers of two different materials with different refractive indexes, and generally is accomplished in a vacuum chamber with each layer taking minutes to deposit. Once a high throughput is needed, or the substrates become larger, it can be quite difficult to make these reflectors to meet these demands.

An alternative is to use chiral nematic (cholesteric) liquid crystals (LCs). A cholesteric liquid crystal (CLC) consists of a LC host material doped with a material with a chiral center, either – right or left-handed. The chiral material causes the subsequent layers of the LC to align such that the director of the LC array is rotated with respect to the previous layer. A right-handed dopant will cause the LC layer to be rotated in a right-handed manner with respect to its neighboring layer. This 'twist' perpetuates through the depth of the LC material, forming a kind of helical structure. The physical distance it takes for the helix to rotate 360 degrees is called the pitch of the helix.

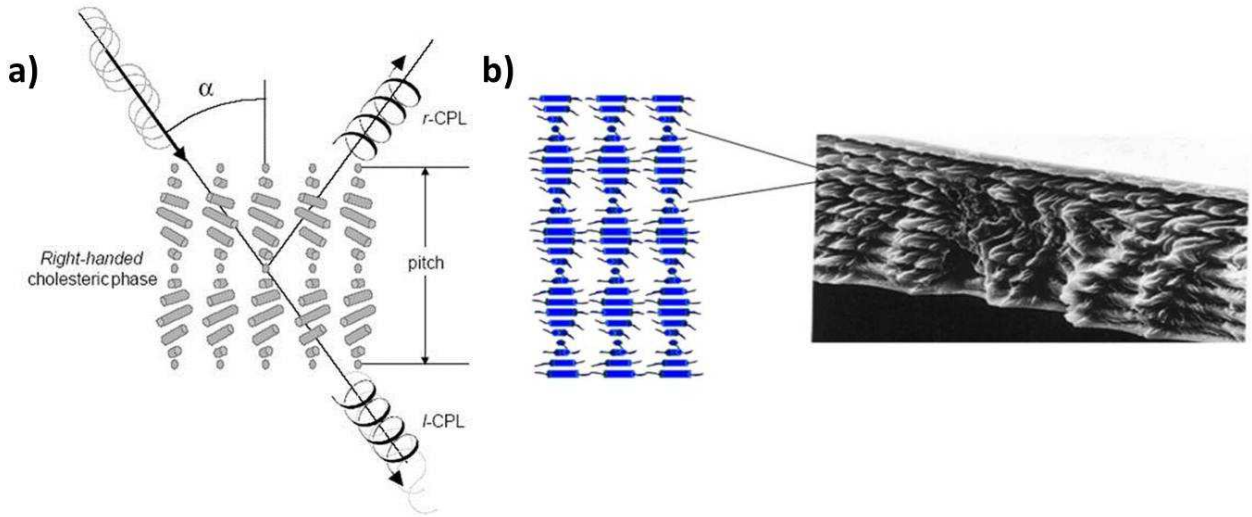

Fig. 18: Diagram defining the pitch and demonstrating the reflection of like-polarized incident light of the matching wavelength, and b) cartoon representation of the stacking of LC layers with a scanning electron microscope edge-on image through the depth of a cholesteric, showing the different layers of the film.

LC monomers are generally long, stiff rods with flexible tails that have a different extraordinary and ordinary refractive index. Through the depth of the LC layer, then, is a periodically changing refractive index, somewhat reminiscent of the bilayer stacks in the inorganic materials. The result of this arrangement is formation of a kind of Bragg reflector, capable of reflecting a narrow bandwidth of light of the same polarization handedness (either right- or left-circularly polarized light: sunlight is a mix of these two polarizations), the bandwidth dependent on the value $\Delta n = n_e - n_o$. Generally, this means the reflectors have a 75 nm bandwidth. We generally use LCs with acrylate tails, allowing us to polymerize the samples after application using ultraviolet light, forming a solid film. The benefits of using cholesterics as the reflector are numerous: they may be deposited directly from solution at low temperatures and self-assemble into the desired structure. Changing the center of the reflection band is done simply by adjusting the amount of chiral dopant added to the LC host.

However, there are disadvantages to using cholesterics as the reflector. The first is that a single layer only reflects one handedness of light, and so a left- and right-handed cholesteric must be stacked on top of each other to achieve full reflection. The second is that the reflection band of the cholesterics is generally too narrow to be used in the device structure as described by the Nanospec project.

In the Nanospec project, the goal was to produce a cholesteric LC reflector broad enough to manage the light. In particular, we were to design a filter capable of reflecting light between both 800 and 1200 nm, and between 1480 and 1600 nm. The approach was to stack a number of narrow band cholesterics together to form a broader band of reflected light.

While a good idea in principle, in practice we discovered some additional challenges. Normally, we produce cholesterics by spin coating on our substrates, which results in films a few microns thick. For reflecting visible light, this is sufficient. However, for infrared reflection, film thicknesses of over 10 microns are required, generally not accessible to spin coating. To get these thicknesses, we tried other deposition techniques such as bar coating and doctor blading, as well as cell filling, but all three methods did not produce reflectors we were satisfied with. In the end, we decided on sequential application of the same material on top of underlying layers to form the reflector. By stacking the individual narrow band reflectors, we achieved quite acceptable broad band reflectors.

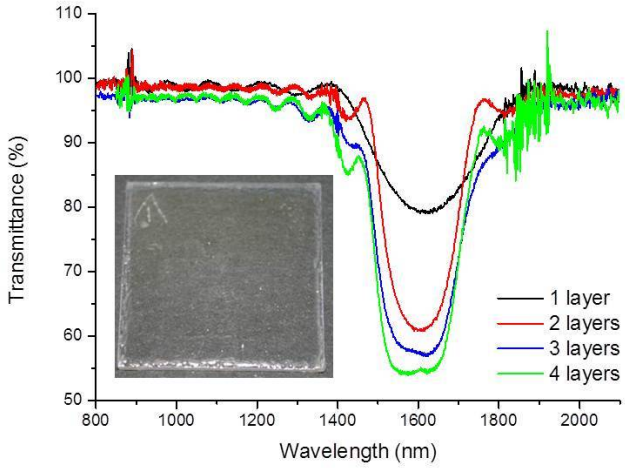

Fig. 19: Transmission resulting from sequential addition of identical right-handed cholesteric layers via spin coating, with a photograph of the completed sample, demonstrating the lack of scatter in the film.

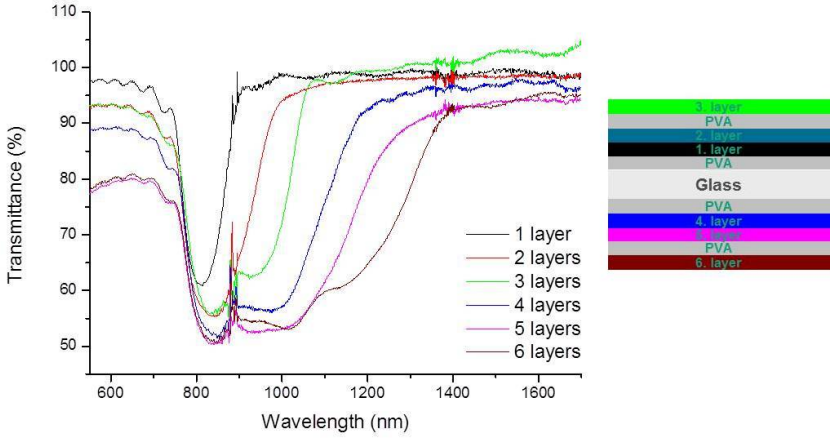

Fig. 20: Transmission spectra of multiple narrow band right-handed reflectors stacked on one object, with diagram showing makeup of final film. Note 'PVA' refers to the polyvinyl alcohol layer used as an alignment layer for the host LC to allow the cholesteric to take a planar form.

However, here we were stymied a bit by the lack of reactive left-handed dopants. Since the left-handed chiral dopant is not physically connected to the rest of the LC host, we found that upon applying the next layer for spin coating, the solvent caused swelling that may have soaked out some of the chiral dopant from the first layer, altering the reflection band. Thus, unless a suitable high-twisting power chiral dopant with left-handed nature can be found, the left-handed reflecting cholesteric will always be of inferior quality.

Initially, the plan was to apply the cholesteric reflectors on top of the device using a simple air gap. However, it was decided during the program it would be desirable to attach the films directly to the substrate. This necessitated that we be able to affix the right- and left-handed reflectors together. We made a rather extensive search of possibilities before obtaining some 'optically clear' double-sided clear tape from 3M Corp. Unfortunately, in attaching the films using this tape the degree of scatter became unacceptably large, so while we were able to produce films with the desired reflection wavelength ranges, we did not create an affixed stack suitable for use in the device structure. Once a suitable lamination method is found to bring the individual reflection foils together, this problem will be solved.

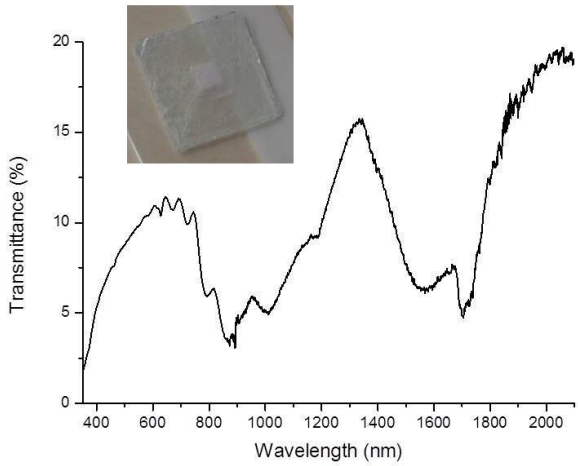

Fig. 21: Transmission spectra of final reflector made using double sided adhesive tape, with a photograph of the final film demonstrating the scattering nature of the layers.

In summary, the desired cholesterics could be produced in principle, but in practice the accelerated timeline and challenges associated with device design did not allow for a final testing of the complete system with the cholesteric reflectors. We have no doubt that in the near future we could produce such an object for testing, and we hope to be able to do so in the context of a follow-up program. We determined that there is actually an advantage in creating infrared cholesteric reflectors, as the average bandwidth of the reflectors increases at longer wavelengths, although it is more difficult to get sharp-edge reflectors due to the very large pitches involved: the layers tend towards a focal conic texture rather than pure planar, and this is exacerbated by the necessity of stacking multiple films.

Embedding of luminescent materials

For the NanoSpec concept, it is not only necessary to develop materials for i) harvesting the near-infrared light that silicon solar cells cannot currently absorb, and ii) up-converting this light to useful wavelengths. It is essential that the novel materials developed by our scientists can be implemented in devices by our engineers. Therefore, the role of this work-package focussed on identifying suitable polymer materials to embed both the micron-size up-conversion (UC) phosphors and near-infrared emitting quantum dots (NQDs) into. The polymer choice is important as it needs to satisfy many optical, chemical, and structural properties. After screening many available polymers, the chosen fluoropolymer was perfluorocyclobutane (PFCB). This particular polymer was chosen due to: i) its excellent optical properties in the range where the up-conversion materials both absorb and emit light; ii) it is rigid enough to be applied as a layer at the rear of the solar cell, and iii) the chemical nature of this polymer has proven to make it a suitable host to the quantum dots. Therefore, this material was chosen as a host for both the UC and NQD materials.

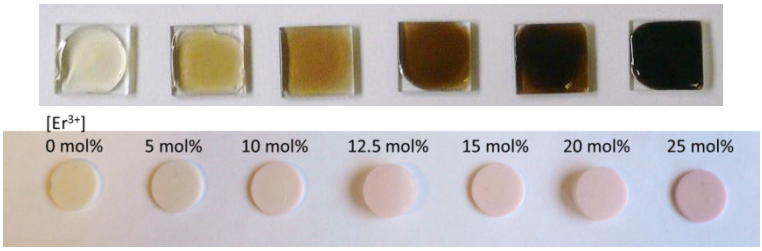

Fig. 22: Photographs of PFCB samples (~1cm across) containing; (top) NQD materials for harvesting near infrared solar energy – black is always a good colour for absorbing sunlight!; (bottom) UC materials based on the "magic" element of erbium (Er^{3+}), which has a characteristic pink colour.

Once the ideal host material was identified, the next step was to determine if the performance of the free-flowing materials developed in earlier workpackages would be maintained after embedding it in the PFCB polymer. Firstly, with the UC phosphors, these materials were not expected to be too sensitive to the choice of polymer and this was confirmed early on in the project. When shining a monochromatic laser onto the UC samples, we measured that up to 8% of the incident light at a wavelength of 1523 nm was being emitted either at 980 nm or even in the red or green region where the human eye is sensitive. The samples that performed best were typically ones that contained 20 – 25% erbium.

However, the sun is not a monochromatic light source – it has a broad spectrum with wavelengths from 300nm (ultraviolet) to 4000nm (infrared) reaching earth. Therefore, our next experiment was to replace the monochromatic light source with a tunable broadband, near infrared one that could be fully absorbed by the erbium ions. The supercontinuum laser that we used as broadband excitation source can be varied to simulate sunlight and also what fraction of this light can be

expected to be absorbed by the erbium UC material. The broadband source yielded even more impressive results of nearly 11% of the photons being up-converted.

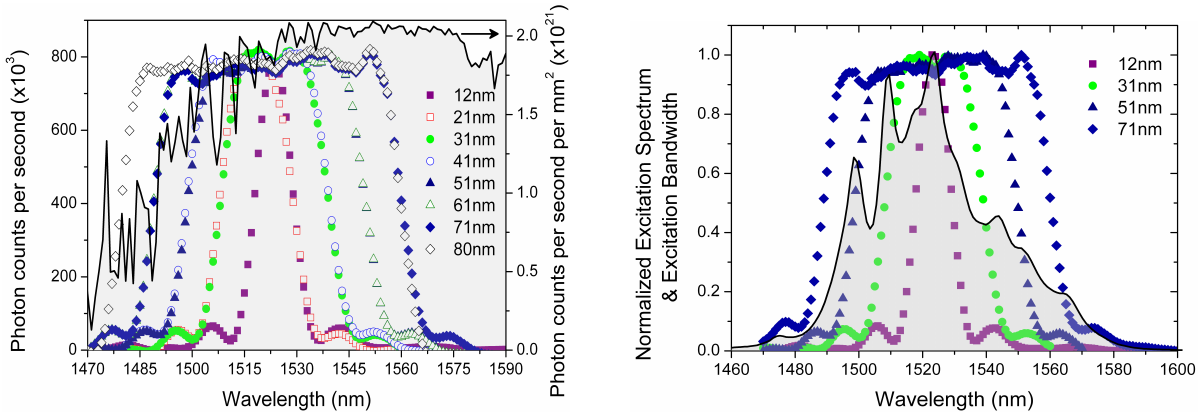

Fig. 23: Graphs showing (left) the variation in broadband excitation (12 – 80nm) that can be achieved with the supercontinuum laser and how it the profile compares to a direct beam of sunlight (shaded grey area); (right) demonstration how four of these bandwidths compare to the absorption profile of the erbium ion that is responsible for UC.

A bandwidth of 60 – 70nm is effectively captured by the erbium UC ions, and there is little point in making the excitation broader and broader as no more light will be absorbed outside the "window" of 1470-1580nm. This is a problem since the silicon solar cell stops absorbing light at about 1150nm, and thus sunlight in the range 1150 – 1470nm cannot be harvested via UC alone. This is the reason for applying the NQD layers in polymer, since they *are* able to absorb light in the range 1150 – 1470nm and emit this again in a region. The efficiency of the NQD materials at emitting light (with respect to the fraction of light absorbed) – a fraction known as the photoluminescent quantum yield (PLQY) – was measured for several samples series. We found that the PLQY strongly depends on the concentration of the NQD material in the polymer, showing a higher efficiency for samples that contained less than 1% NQDs. The highest PLQY value obtained was ~20% for NQDs that were based on a lead selenide (PbSe) and lead sulphide (PbS) material system. NQDs where the PbS layer is instead replaced by cadmium selenide (CdSe) exhibit a similar PLQY of around 18%.

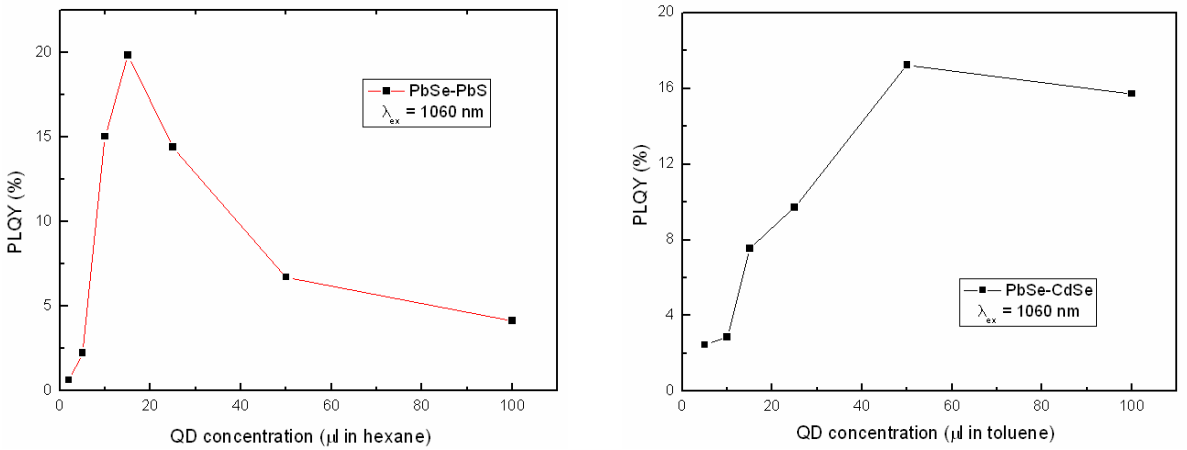

Fig. 24: Graphs showing the variation in measured PLQY as a function of the NQD concentration in the PFCB polymer layers: (left) PbSe-PbS NQDs, and (right) PbSe-CdSe NQDs

There is, however, a relatively large region of overlap between the NQD absorptions and its emission in the region from 1400 – 1500nm, which results in reduced light emission. Thus, when thicker layers were measured using broadband excitation (1180 – 1230 nm) the resulting PLQY values were lower – typically in the range of 7% for PbSe-CdSe NQDs and 14% for PbSe-CdSe NQDs.

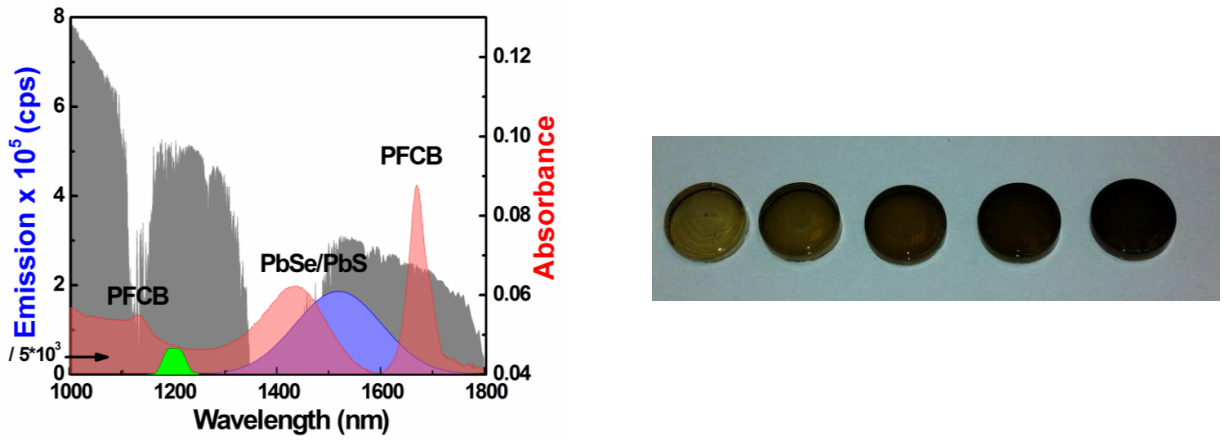

Fig. 25: (left) Absorbance (red curve), emission (blue curve) and the broadband excitation (green curve) spectra of a typical PFCB sample containing PbSe/PbS NQDs (shown on right). For comparison the direct solar spectrum is also shown (gray shaded region).

A special way of embedding the upconverter material is in micro-resonator structures. The idea is to increase the upconversion efficiency, by a) increasings the irradiance on the upconverter at the excitation wavelength of 1523 nm and b) increasing emission at the wanted emission wavelength of 980 nm. The increase of the irradiance was achieved with a filter behind the upconverter, which was designed to be highly reflective at 1523 nm. Additionally, two additional filters that are reflective at 980 nm form a resonant cavity for this wavelength around the upconverter layer.

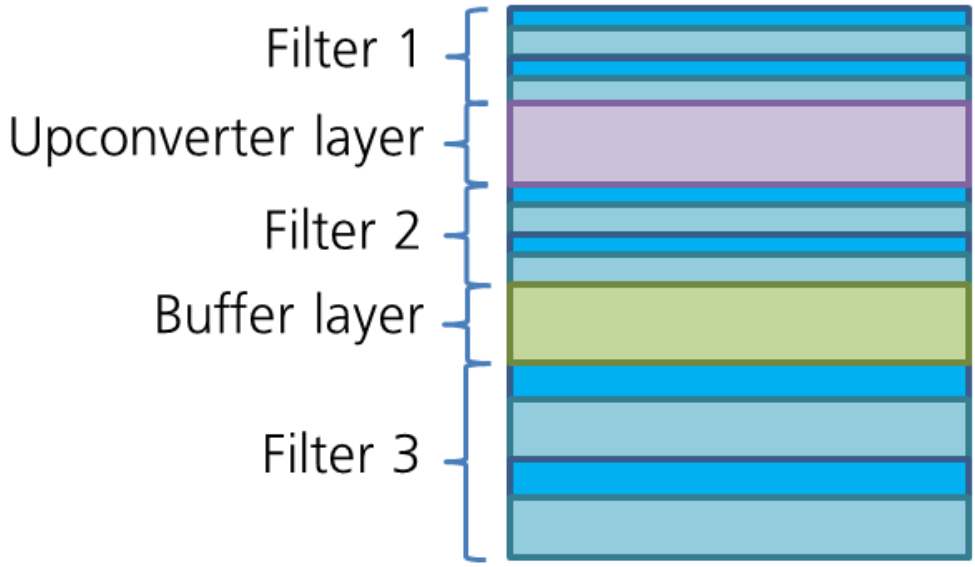

Fig. 26: Schematic design of the micro-resonator structure. Filter 3 reflects the incoming light at around 1523 nm, Filter 1 and 2 form a resonant cavity for the wanted emission around 980 nm.

Using the previously described spectrally selective photonic structures, coated with an upconverter layer, such micro-resonator structures were realized. It proved quite an experimental challenge to combine the two filter structures and the upconverter layer to one final system. Different approaches were tested for this purpose. Finally, pressing under heat in an evacuated system was successful. The upconversion photoluminescence (PL) of several samples could be measured. We found that the upconversion PL was nearly tripled when the upconverter layer was deposited on the back filter structure instead of a bare substrate. Forming a complete cavity, however, did not improve the PL any further.

Fabrication of bifacial silicon solar cells

In the Nanospec project, bifacial solar cells were produced from n-type, mono-crystalline silicon. Their most striking features were optimized double layer anti-reflection coatings on the front, and a single layer anti-reflection coating at the rear. These layers should ensure several things: a) light that can be directly used by the solar cell should not be reflected, b) light that can be used by the upconverter should be transmitted through the solar cell and c) light that is emitted by the upconverter should enter the solar cell. Indeed, a high external quantum efficiency (EQE) was achieved for illumination from the front, and a high EQE was achieved around 980 nm for illumination from the rear. Furthermore, also high transmission of upconvertible light was realized.

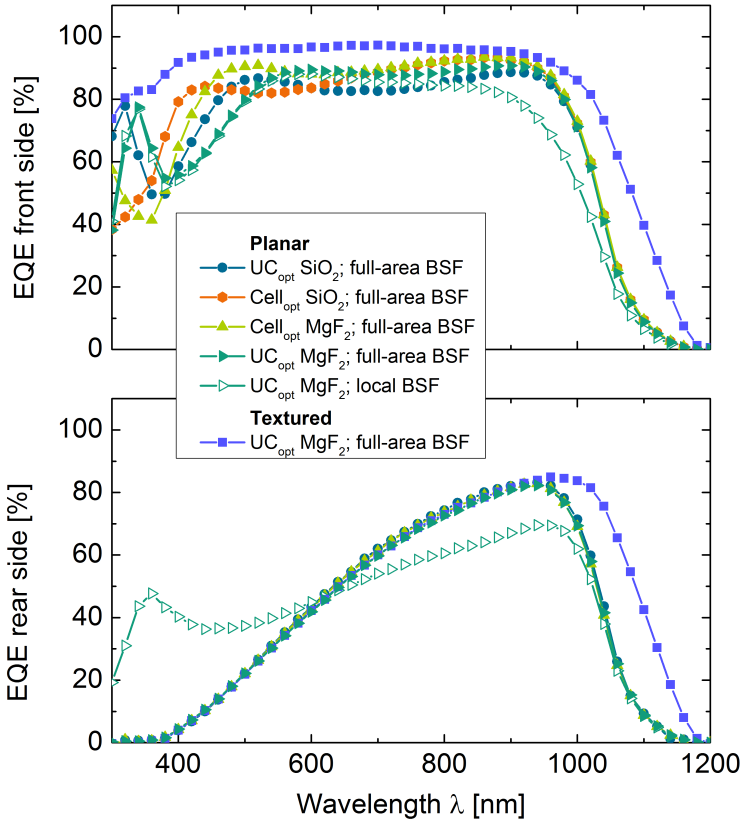

Fig. 27: EQE measurements from front and rear, showing the adapted bifacial functionality.

Furthermore, microcrystalline silicon thin-film solar cells were deposited on front electrodes with enhanced transparency achieved by an adapted TCO annealing processes developed in the first period. In order to mitigate resistive losses arising from the annealing, metal grid configurations were developed and optimized via modelling. In combination with a retro-reflector foil applied to reduce shading losses due to the contact grid, the performance of fully metalized back contact solar cells could be increased beyond the control sample with unoptimized front. In a second step,

the full metallization of the back contact was replaced by a grid design to allow for the required outcoupling of the NIR spectra. Both grid spacing and TCO design parameters were again analyzed computationally. At the end of the project, thin film silicon solar cells with enhanced NIR transparency due to optically optimized front and back contacts have been fabricated, which allowed for the measuring of NIR up-conversion in these cells, with only a minimal degradation of the overall cell performance under standard illumination conditions.

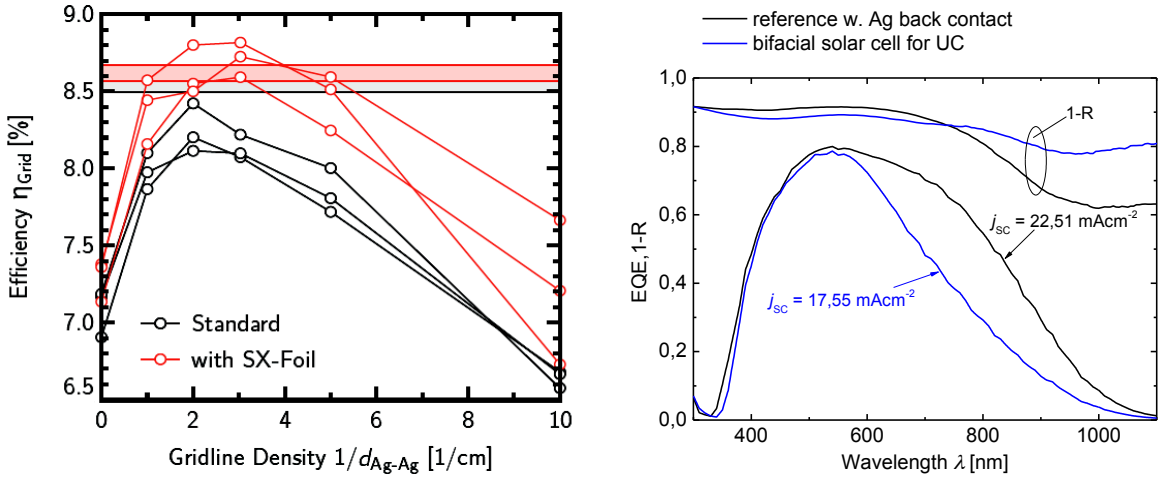

Fig. 28: (Left) Performance of microcrystalline silicon solar cells on annealed ZnO front contact with grid configuration and full back contact metallization (black circles), as compared to cells with standard electrode (horizontal black line); the application of a retroreflector foil to reduce the shading losses gives rise to an enhanced efficiency (red circles). (Right) EQE of fully optimized bifacial solar cell exhibits equivalent performance in the visible and enhanced transparency in the NIR.

Realization of upconverter solar cell devices

The different components of the Nanospec system, the solar cells, the embedded upconverter, the embedded NQD and the photonic structures were combined to upconverter solar cell devices and extensively characterized under monochromatic and broad-band excitation. No positive effect on the system efficiency was found for the embedded NQD. Therefore, the most optimised system was realised with only a mono-crystalline silicon solar cell and embedded upconverter material. For this system, record values were achieved in terms of the systems external quantum efficiency in respect to the excitation intensity. Overall, due to the achievements of the Nanospec project in solar cell and material development, the efficiency could be increased by a factor of six in comparison with older values.

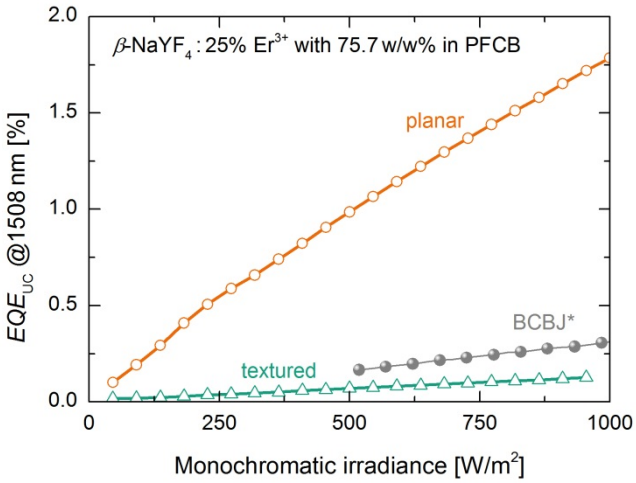

Fig. 29: The EQE_{UC} of a planar solar cell could be increased by a factor of around 6, compared to the older reference case (BCBJ) by optimizing the transmittance of the solar cell and due to a more efficient upconverter. For the front side textured solar cells the effect of the upconverter is fairly low, because of the poor transmittance.

For an upconverter solar cell device, in which β-NaYF4 : 25% Er^{3+} embedded in PFCB with a powder to polymer concentration of 75.7 w/w% was coupled to the solar cell, an additional short-circuit current density due to upconversion of sub-band-gap photons $\Delta J_{SC,UC}$ of 2.2 ±0.3 mA/cm^2 was determined under broadband excitation ranging from 1450 nm to 1600 nm and an equivalent solar concentration of 78±6 suns.

The upconverter solar cell devices, were finally integrated into concentrator module like structures, featuring a 10 cm x 10 cm Fresnel lens. These modules were than characterized both in a solar simulator setup and outdoors, mounted a solar tracking unit. Again record efficiency values were obtained and significant effects on the short-circuit current density were already observed for comparatively low concentration factors. In solar simulator measurements a $\Delta J_{SC,UC}$ of 13.3 ±3.0 mA/cm^2 was achieved for a concentration of 207±86 suns. This is the highest $\Delta J_{SC,UC}$ value determined so far.

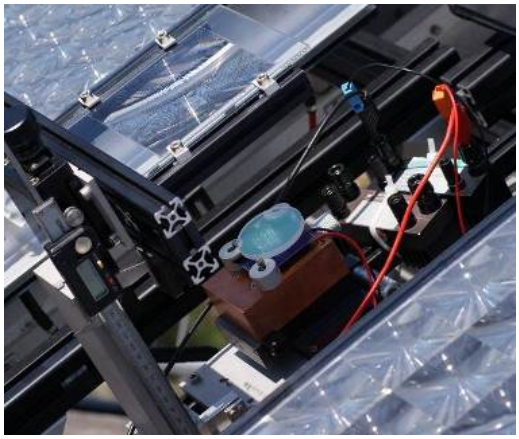

Figure 30: Concentrator module in the outdoor test setup. By changing the height of the lens above the solar cell upconverter device the concentration of the solar radiation can be altered.

Impact

Socio-Economic Impact

For the successful development of the Nanospec concept into products with huge impact, it is necessary to keep in mind the abundance and toxicity of the materials involved, as well as the energy and cost economy of the products. The important materials involved in this project are the near-infrared emitting quantum dots (QD) and the UC phosphors QDs [e.g. lead selenide – cadmium selenide (PbSe-CdSe) and lead selenide – lead sulfide (PbSe-PbS) core-shell quantum dots and the corresponding alloys] used in the present project are based on elements lead, cadmium, sulphur and selenium. These elements are relatively abundant in the earth‘s upper continental crust as compared to the common noble metal gold. One of the important constituents of the UC phosphors are the rare-earth (RE) elements. RE elements, as the name might suggest, are however not ‘rare’ but relatively abundant in the Earth‘s crust, some even more abundant than copper, gold, and platinum. However, in contrast to ordinary base and precious metals, RE elements are not often found in concentrated and economically exploitable minerals. It was the very scarcity of these minerals that led to the term "rare earth". China has a near-monopoly position in world RE production (and is the dominant RE supplier of the raw material, downstream oxides, associated metals and alloys) but continues to restrict exports of the material through quotas and export tariffs. As China continues to restrict the RE exports, the US, Europe, Japan, Canada, Australia, and India are all endorsing efforts to start/re-open more RE mines. Substitution efforts, which replace critical minerals of unreliable supply, with easier to find materials, and recycling are also being considered worldwide.

In general, the toxicity of RE decreases as the atomic number increases and is related to the greater solubility and ionic stability of the heavier RE. And the most important aspect of QD toxicity is their stability, both *in vivo* and during synthesis and storage. Several studies suggest QD cytotoxicity to be due to photolysis or oxidation. Under oxidative and photolytic conditions, QD core–shell coatings have been found to be labile, degrading and thus exposing potentially toxic capping material or intact core metalloid complexes or resulting in dissolution of the core complex to QD core metal components.

However since in the present study, both the UC phosphors as well as QDs are embedded in polymers the samples are safer to handle as well as to machine. To make an assessment of the potential release of particles into the working environment resulting from the machining of the quantum dot-based polymer samples using a lathe, detailed studies on nanoparticle monitoring were carried out as part of Nanospec. The potential surface contamination by process materials was also investigated. From these detailed investigation it was concluded that no significant release of sub-µm respirable particles or larger particles (100 nm – 20 µm) into the workplace atmosphere during the machining of the quantum dot-containing polymer. Measurements within

the activity zone and breathing zone were similar and did not detect any significant deviation in particle concentration from the typical background, with the vacuum extraction either on or off. To evaluate the energy effectiveness of the Nanospec concept, the energy pay back time (EPBT) of a concentrating PV system with the Nanospec PV devices has been estimated.

EPBT is defined as the time (in years) in which the energy input during the module life-cycle is compensated by electricity generated by the PV module. The energy payback time for 24 kW Amonix HCPV system with each solar cell replaced with the simplified Nanospec PV devices has been found to be 2.7 years as compared to the standard reference device with 3.7 years. The primary purpose for using concentrating PV systems is to capture the maximum amount of sunlight and focus it on to a small cell area, thereby ultimately reducing the cost of high-efficiency solar-cell materials.

Additionally, studies on cost efficiency of the proposed concept have also been carried out. An existing costing model for solar cells was used to create different reference cost scenarios. These reference cases were used to calculate allowable extra costs for projected and achieved efficiency enhancements due to upconversion. These figures were compared with a bottom up calculation of the additional costs of a Nanospec system. As in the past the NQD had been the most costly component, a detailed cost calculation based on the progresses of the synthesis procedure developed in Nanospec was performed. Our calculations showed that for a solely Erbium based system, cost efficiency could be achieved in high concentrating systems, but only for those. The addition of efficient NQD would increase the cost competiveness considerably. That is, when in further developments of the Nanospec technology, the overall system efficiency is further increased, a significant contribution to lower costs of concentrator photovoltaic technology could be achieved, helping the more widespread dissemination of solar electricity generation.

The technology developed in Nanospec is, however, not close to introduction into the photovoltaic market yet. Nevertheless, the wide range of successful Nanospec results offers several opportunities for exploitation. The developed synthesis approaches, especially the high chemical yield processes for luminescent NQDs could be used to produce materials, which in turn are used in research. Several companies exist that sell luminescent NQD to research institutions for various purposes. The developed upconverter materials could be used in medical imaging with IR excitation and NIR emission in an optical window that is favorable for bio-imaging. The highly efficient IR-NIR UC materials may also be applied as invisible labels for anti-counterfitting. Spectrally selective photonic structures can find use as IR reflectors to maintain interior temperatures by rejecting solar heating from a room space. The spectral range of the infrared in sunlight spans from 750 nm to over 4000 nm, so the broader the range, the more control one can have. Transparency is very important, and the techniques used in Nanospec are useful in developing the processing conditions necessary to produce such reflectors with appropriate characteristics.

Dissemination

The results of Nanospec were disseminated in more than 20 publications in peer-reviewed journals. Reflecting the excellence of the work within Nanospec, publications were accepted in high-impact journals leading in the respective fields, like Nano Lett, Small, Chemistry of Materials, Physical Review B, New Journal of Physics, Optics Express, and Solar Energy Materials and Solar Cells. This range of different journals also reflects the inter-disciplinarity of the research performed in Nanospec, ranging from material research to solar cell device fabrication.

Furthermore, 48 presentations were given at conferences and workshops on results of Nanospec. Several of those were invited talks or plenary lectures. Stefan Fischer, a PhD student at Fraunhofer ISE very actively involved in the Nanospec activities won the best student presentation award at the IEEE photovoltaic conference 2013, for a presentation in which he communicated important results that were obtained on the material and system characterization level as part of Nanospec. This prize is reflecting the high quality of both the performed research and the supervision and dissemination activities. To honour the award Fraunhofer ISE released a press information, explicitly stating Nanospec and the involved partners.

On the 21st and 22nd of February 2013, a "workshop on advanced systems for photon management for photovoltaics", with a special focus on upconversion took place in Freiburg at the Fraunhofer Institute for Solar Energy Systems ISE. 38 international guests including the Nanospec project partners, researchers from different relevant fields and representatives from industry all contributed to the workshop being a big success.

PhD students, Master students and student research assistants have actively participated in the research of the nanospec-project at most project partners. The principal investigators at each institution supervised these students and helped them to develop their scientific knowledge and their professional skills.

Table I: List of publications of the Nanospec project in peer-reviewed journals and books.

Title	Main Author (Institution)	Journal	Issue	Publisher	Place of Publication	Date of publication	Pages	Permanent identifier	Open Access (yes/no)
Two-Fold Emission From the S-Shell of PbSe/CdSe Core/Shell Quantum Dots	D. Grodzińska (UU)	Small	7(24)	Wiley-VCH Verlag	Weinheim	21/10/2011	3493-3501	10.1002/smll.201101819	Yes
Anomalous Independence of Multiple Exciton Generation on Different IV-VI Quantum Dot Architectures	E.Lifshitz (TEC)	Nano Lett.	**11**(4)	American Chemical Society	Washington, DC	24/02/2011	1623-1629	10.1021/nl200014g	Yes
Origin of the high upconversion green luminescence efficiency in β-$NaYF_4$:2%Er^{3+}, 20%Yb^{3+}	C. Renero-Lecuna (UBE)	Chemistry of Materials	23(15)	American Chemical Society	Washington, DC	06/07/2011	3442-3448	10.1021/cm2004227	NoPre
Photonic structures for a solar cell upconversion system	B.Herter (ISE)	Future PV	6	Mazik Media Inc.	Mill Valley, DC	01/12/2011	55-61	10.1117/12.922490	Yes
Experimental analysis of upconversion with both coherent monochromatic irradiation and broad spectrum illumination	J.C. Goldschmidt (ISE)	Solar Energy Materials and Solar Cells	95(7)	Elsevier	Oxford, UK	23/02/2011	1960-1963	10.1016/j.solmat.2011.01.019	No
Plasmon enhanced upconversion luminescence near gold nanoparticles–simulation and analysis of the interactions	S. Fischer (ISE)	Optics Express	20(1)	Optical Society of America	Washington, DC	02/01/2012	271–282	10.1364/OE.20.000271	No
Use of NIR light and upconversion phosphors in light-curable polymers	A. Stepuk (UBE)	Dental Mater.	28	Elsevier	Oxford, UK	01703/2012	304-311	10.1016/j.dental.2011.11.018	No
Fluorescence of colloidal PbSe/PbS QD in NIR luminescent solar concentrators	U. Aeberhard (IEF)	Phys. Chem. Chem. Phys	14(47)	RSC Publishing	Cambridge, UK	14/12/2012	16223-16228	10.1039/c2cp42213a	No
High-Temperature Luminescence Quenching of Colloidal Quantum Dots	W. Evers (UU)	ACS Nano	6 (10)	American Chemical Society	Washington DC	14/09/2012	9058-9067	10.1021/nn303217q	Yes
Highly efficient IR to NIR upconversion in Gd2O2S: Er3+ for photovoltaic applications	R. Martin Rodriguez (UU)	Chemistry of Materials	25	American Chemical Society	Washington DC	05/04/2013	1912–1921	10.1021/cm4005745	Yes
Ultra-high photoluminescent quantum yield of β-NaYF4: 10% Er3+ via broadband excitation of upconversion for photovoltaic devices	S.W. MacDougall (HWU)	Optics Express	S6	Optical Society of America	Washington, DC	09/10/2012	A879-A887	10.1364/OE.20.00A879	Yes
Optimizing infrared to near infrared upconversion quantum yield of β-NaYF4:Er3+ in fluoropolymer matrix for photovoltaic devices	A.Ivaturi (HWU)	Journal of Applied Physics	1	American Institute of Physics	Melville, NY	03/07/2013	013505(1-9)	10.1063/1.4812578	No

Alloy and heterostructure architectures as promising tools for controlling electronic properties of semiconductor quantum dots	E.Lifshitz (TEC)	Phys. Rev. B	85	American Physical Society	USA	02/02/2012	075304	10.1103/PhysRevB.85.075304	yes
Influence of alloying on the optical properties of IV-VI Nanorods	E.Lifshitz (TEC)	Journal of Physical Chemistry C	116(35)	American Chemical Society	USA	01/08/2012	18983–18989	10.1021/jp303200b	no
Increasing upconversion by plasmon resonance in metal nanoparticles – a combined simulation analysis	J.C.Goldschmidt (ISE)	IEEE JPV	2 (2)	IEEE	USA	23/02/2012	134-140	10.1109/JPHOTOV.2011.2182179	yes
Modeling upconversion of erbium doped microcrystals based on experimentally determined Einstein coefficients	S. Fischer (ISE)	JAP	111(1)	American Institute of Physics	USA	19/01/2012	013109 - 013109-13	10.1063/1.3674319	yes
The Influence of Alloy Composition on the Electronic Properties of IV–VI Core/Shell Colloidal Heterostructures	E.Lifshitz (TEC)	Isr. J. Chem	52	Wiley-VCH Verlag GmbH&Co. KGaA,	Weinheim, Germany	03/12/2012	1037 – 1052	10.1002/ijch.201200068	yes
Tuning of Electronic Properties in IV–VI Colloidal Nanostructures by Alloy Composition and Architecture	E.Lifshitz (TEC)	Nanoscale	12	RSC Publishing	Beijing, China	In press-July 2013		10.1039/C3NR02141F.	yes
Stark level analysis of the spectral line shape of electronic transitions in rare earth ions embedded in host crystals	Steinkemper (ISE)	New Journal of Physics	15	IOP Publishing Ltd	Bristol, UK	21/05/ 2013	053033	10.1088/1367-2630/15/5/053033	yes
Solar Spectrum Conversion for Photovoltaics Using Nanoparticles	W. van Sark (UU)	Book Chapter		InTech	New York	01/03/2012		ISBN 978-953-51-0304-2, DOI: 10.5772/39213.	Yes
Temperature-dependent optical properties of colloidal IV-VI quantum dots, composed of core/shell heterostructures with alloy components	E.Lifshitz (TEC)	Book "Quantum Dots"	Chapter 3	InTech	Croatia	13/06/2012	63-90	10.5772/35048	yes
Photonics for Photovoltaics	J.C. Goldschmidt (ISE)	European Energy Innovation	Spring 2013	Prologue Media	Hertfordshire, UK	2013	36		yes